OXFORD

SOT | Society of Toxicology
www.toxsci.oxfordjournals.org

TOXICOLOGICAL SCIENCES, 169(2), 2019, 333–352

doi: 10.1093/toxsci/kfz049
Advance Access Publication Date: February 22, 2019
Research Article

Mechanistic Interplay Between Autophagy and Apoptotic Signaling in Endosulfan-Induced Dopaminergic Neurotoxicity: Relevance to the Adverse Outcome Pathway in Pesticide Neurotoxicity

Chunjuan Song,[1] Adhithiya Charli,[1] Jie Luo, Zainab Riaz, Huajun Jin, Vellareddy Anantharam, Arthi Kanthasamy, and Anumantha G. Kanthasamy[2]

Department of Biomedical Sciences, Iowa Center for Advanced Neurotoxicology, Iowa State University, Ames, Iowa 50011

[1]These authors contributed equally to this study.
[2]To whom correspondence should be addressed at Parkinson's Disorder Research Laboratory, Department of Biomedical Sciences, Iowa Center for Advanced Neurotoxicology, 2062 Veterinary Medicine Building, Iowa State University, Ames, IA 50011, USA. Fax: 01-515-294-2315. E-mail: akanthas@iastate.edu.

ABSTRACT

Chronic exposure to pesticides is implicated in the etiopathogenesis of Parkinson's disease (PD). Previously, we showed that dieldrin induces dopaminergic neurotoxicity by activating a cascade of apoptotic signaling pathways in experimental models of PD. Here, we systematically investigated endosulfan's effect on the interplay between apoptosis and autophagy in dopaminergic neuronal cell models of PD. Exposing N27 dopaminergic neuronal cells to endosulfan rapidly induced autophagy, indicated by an increased number of autophagosomes and LC3-II accumulation. Prolonged endosulfan exposure (>9 h) triggered apoptotic signaling, including caspase-2 and -3 activation and protein kinase C delta (PKCδ) proteolytic activation, ultimately leading to cell death, thus demonstrating that autophagy precedes apoptosis during endosulfan neurotoxicity. Furthermore, inhibiting autophagy with wortmannin, a phosphoinositide 3-kinase inhibitor, potentiated endosulfan-induced apoptosis, suggesting that autophagy is an early protective response against endosulfan. Additionally, Beclin-1, a major regulator of autophagy, was cleaved during the initiation of apoptotic cell death, and the cleavage was predominantly mediated by caspase-2. Also, caspase-2 and caspase-3 inhibitors effectively blocked endosulfan-induced apoptotic cell death. CRISPR/Cas9-based stable knockdown of PKCδ significantly attenuated endosulfan-induced caspase-3 activation, indicating that the kinase serves as a regulatory switch for apoptosis. Additional studies in primary mesencephalic neuronal cultures confirmed endosulfan's effect on autophagy and neuronal degeneration. Collectively, our results demonstrate that a functional interplay between autophagy and apoptosis dictate pesticide-induced neurodegenerative processes in dopaminergic neuronal cells. Our study provides insight into cell death mechanisms in environmentally linked neurodegenerative diseases.

Key words: autophagy; apoptosis; PKCδ; pesticides; Parkinson's disease; neurotoxicity.

The etiopathogenesis of Parkinson's disease (PD) still remains unclear. Nevertheless, increasing evidence suggests that environmental risk factors, such as exposure to heavy metals and pesticides, may be significantly related to the development of idiopathic PD (Brown *et al.*, 2006; Fleming *et al.*, 1994; Fleming, 2017; Hatcher *et al.*, 2007, 2008; Jia and Misra, 2007a; Kanthasamy *et al.*, 2005, 2012; Richardson *et al.*, 2006; Tanner and Ben-Shlomo, 1999). The cellular and molecular mechanisms of environmental neurotoxic stress-induced dopaminergic neurodegeneration have been intensively studied for several decades, yet the key signaling mediators responsible for regulating the neurodegenerative process are yet to be established.

Pesticides make up a large and growing group of chemicals that induce neurotoxic effects. Endosulfan (6,7,8,9,10,10-hexachloro-1,5,5a,6,9,9a-hexahydro-6,9-methano-2,4,3-benzodioxathiepin-3-oxide) is an organochlorine insecticide that has been widely used in agriculture and forestry around the world. However, endosulfan can adversely affect nontarget organisms due to its long persistence in the environment and high potential to bioaccumulate in the tissues of fish and mammals, including humans. Endosulfan can even be detected and involved in the toxicity of some aquatic and terrestrial wildlife (Aleksandrowicz, 1979; Blanco-Coronado *et al.*, 1992; Boereboom *et al.*, 1998; Brandt *et al.*, 2001; Chan *et al.*, 2006; Demeter *et al.*, 1977; Eyer *et al.*, 2004; Kelly and Gobas, 2003; Kim *et al.*, 2018; Kumari *et al.*, 2016; Oliveira *et al.*, 2017; Ribeiro *et al.*, 2001). Moreover, endosulfan residues have been detected in the brains of orally administered rats (Ansari *et al.*, 1984; Dikshith *et al.*, 1984; Gupta, 1978; Jang *et al.*, 2016; Lafuente and Pereiro, 2013; Zervos *et al.*, 2011). In humans, neurotoxicity and psychiatric syndromes, including tremor, epilepsy, hyperactivity, irritability, paralysis, and memory defects, have been reported in industrial or agricultural workers suffering from acute exposure to endosulfan (Agrawal *et al.*, 1983; Aleksandrowicz, 1979; Kucuker *et al.*, 2009; Naqvi and Vaishnavi, 1993; Paul *et al.*, 1994; Silva and Gammon, 2009). Reflecting these significant risks, the United States Environmental Protection Agency (EPA) banned the use of endosulfan in 2010 (Lubick, 2010). To date, endosulfan has been phased out in 62 countries, but it still poses an environmental exposure risk for humans due to its long environmental half-life (Menezes *et al.*, 2017; Silva and Gammon, 2009).

Previous studies show that exposure to endosulfan induces cytotoxicity and apoptosis in various cell types, including neuronal cells, via oxidative stress and mitochondrial dysfunction, which is mostly known to involve disruption of the mitochondrial transmembrane potential (Du *et al.*, 2015; Jia and Misra, 2007b,c; Kang *et al.*, 2001; Kannan *et al.*, 2000; Kannan and Jain, 2003; Lakroun *et al.*, 2015; Wang *et al.*, 2012). Exposure to endosulfan also proved cytotoxic to rat and human neuronal and glial cells (Brown *et al.*, 2006; Chan *et al.*, 2006; Seth *et al.*, 1986). Dopaminergic neurons are particularly sensitive to endosulfan-induced neurotoxicity in both cell culture and animal models of PD (Brown *et al.*, 2006; Chan *et al.*, 2006; Seth *et al.*, 1986; Wilson *et al.*, 2014), and reports of endosulfan-induced hyperactivity and circling movements (Ansari *et al.*, 1987; Chhillar *et al.*, 2013; Paul and Balasubramaniam, 1997; Wilson *et al.*, 2014) suggest an increased risk of PD. This hypersensitivity of dopaminergic receptors to endosulfan was indicated in another study demonstrating that endosulfan can significantly reduce the number of striatal dopaminergic receptors in rats without affecting other receptor profiles (Seth *et al.*, 1986).

Despite the adverse effects of endosulfan and its established link with neurotoxicity (Gude and Bansal, 2012; Lee *et al.*, 2015; Wilson *et al.*, 2014), the biochemical and cellular mechanisms of endosulfan-caused dopaminergic neurotoxicity have been understudied and are still largely unknown. Autophagy, one of the major pathways for the degradation of intracellular macromolecules, is usually triggered in response to adverse environmental conditions, such as starvation, infection, hypoxia, radiation and numerous cytotoxic stimuli (Ding *et al.*, 2007; Klionsky and Emr, 2000). It has been shown recently that endosulfan contributes significantly to triggering autophagy by generating oxidative stress (Rainey *et al.*, 2017; Zhang *et al.*, 2017b). Autophagy plays a fundamental role in neuronal homeostasis and survival and its dysregulation has been linked to neurodegenerative diseases (Lee, 2009; Nixon, 2006; Winslow and Rubinsztein, 2008; Wong and Cuervo, 2010). Here, we show for the first time that endosulfan exposure resulted in autophagy in dopaminergic neuronal cells, followed by apoptotic cell death. Our findings (1) indicate that endosulfan-induced autophagy may act as an early survival mechanism against the later-onset apoptosis-driven degeneration of dopaminergic neuronal cells and (2) imply that autophagy dysfunction plays a central role in the etiology of PD. Thus, the search for an efficacious autophagy enhancer could be integrated into the development of potential PD therapies.

MATERIALS AND METHODS

Chemicals and reagents. Endosulfan (purity 73.2%) was obtained from Chem Service Inc. (West Chester, Pennsylvania). Wortmannin and bafilomycin A1 were purchased from Sigma Chemical Co. (St. Louis, Missouri). The caspase-2 substrate Ac-VDVAD-AFC and specific inhibitor Z-VDVAD-fmk, caspase-3 substrate Ac-DEVD-AFC and specific inhibitor Z-DEVD-fmk, caspase-8 substrate Ac-IETD-AFC, and caspase-9 substrate Ac-LEHD-AFC were obtained from Bachem Biosciences (King of Prussia, Pennsylvania). The substrate used to examine proteasomal activity, Suc-Leu-Leu-Val-Try-7-amino-4-methylcoumarin-AMC (Suc-LLVY-AMC), was purchased from Calbiochem (San Diego, California). The Cell Death Detection enzyme-linked immunosorbent (ELISA) Plus assay kit was purchased from Roche Molecular Biochemicals (Indianapolis, Indiana). RPMI 1640 medium, fetal bovine serum, L-glutamine, penicillin/streptomycin, and SYTOX green dye were purchased from Invitrogen (Carlsbad, California). The Bradford protein assay kit was purchased from Bio-Rad (Hercules, California). The primary antibodies used in this study were Beclin-1, caspase-2, caspase-3, PKCδ (catalog no. sc-11427, sc-625, sc-7148, respectively) (1:1000, rabbit polyclonal, Santa Cruz Biotechnology, Santa Cruz, California), cytochrome c (catalog no. MAB 1800) (1:1000, mouse monoclonal, Millipore, Billerica, Massachusetts), β-actin (catalog no. A2228) (1:10000, mouse monoclonal, Sigma), ubiquitin (catalog no. Z0458) (1:2000, rabbit polyclonal antibody, DakoCytomation California Inc., Carpinteria, California), phospho-PKCδ (T505) (catalog no. sc-11770) (1:1000, Goat polyclonal antibody, Santa Cruz Biotechnology), LC3 (catalog no. 2775), and cleaved caspase-3 (A175) (catalog no. 9664) (1:1000, rabbit monoclonal, Cell signaling, Danvers, Massachusetts). IR Dye 800-conjugated anti-rabbit (1:10000) (Rockland labs, Gilbertsville, Pennsylvania) and Alexa Fluor 680 conjugate anti-mouse (1:10000) (LI-COR, Lincoln, Nebraska) secondary antibodies were used.

Cell culture and CRISPR/Cas9-based knockout of PKCδ in N27 cells. Immortalized rat mesencephalic/dopaminergic cells (N27 cells) were grown in RPMI 1640 medium containing 10% fetal bovine serum, 2 mM L-glutamine, 50 units penicillin and 50 μg/ml

streptomycin and incubated at 37°C in a humidified atmosphere containing 5% CO_2. Two-to-three-day old cells were used for experiments. Primary mesencephalic neuronal cultures were prepared from the dissected brains of timed-pregnant C57BL/6 mice (gestation E14) as described previously (Zhang et al., 2007). Briefly, fetal mesencephalic tissues were maintained in ice-cold Ca^{2+}-free HBSS and then the cells were dissociated in HBSS solution containing trypsin-EDTA (0.25%) for 30 min at 37°C. Next, the dissociated cells were seeded at equal density (1×10^6 cells) in 30-mm diameter tissue culture wells that were pre-coated with poly-D-lysine (1 mg/ml) and 10 μg/ml laminin. Cultures were maintained in neurobasal medium fortified with B-27 supplements, L-glutamine (500 μM), penicillin (100 IU/ml), and streptomycin (100 μg/ml) (Invitrogen). The cells were incubated for 6–7 days at 37°C in a humidified atmosphere of 5% CO_2. Half of the culture medium was replaced every 2 days.

To make lentivirus, the lentivirus-based CRISPR/Cas9 PKCδ KD plasmid pLVU6gRNA-Ef1aPuroCas9GFP-PKCδ with the PKCδ gRNA target sequence GCGTCGTCCTCCGCCTGCAGGG (Sigma-Aldrich) and control plasmid were transfected into 293FT cells using the Mission Lentiviral Packaging Mix (SHP001; Sigma-Aldrich) according to the manufacturer's instructions. The lentivirus was harvested 48 h post-transfection and titers were measured using the Lenti-X p24 Rapid Titer kit (Clontech, Mountain View, California). For stable KD of PKCδ in N27 cells, 6-well plates containing 0.1×10^6 cells/well had lentivirus added the following morning to the media at an MOI of 100. After 24 h, fresh media supplemented with puromycin (50 μg/ml) was added to the cells for stable cell selection.

Plasmid constructs. The GFP-LC3 and GFP-LC3-ΔG constructs were kind gifts from Dr Isei Tanida, National Institute of Infectious Disease, Japan. GFP-LC3-ΔG is a mutant whose C-terminal Glycine, which is essential for lipidation, was deleted. This construct was used as a negative control to identify lipidation-independent LC3 puncta.

SYTOX cell death assay and morphometric studies. Cell death was examined under phase-contrast microscopy and determined by SYTOX green assay as described previously (Afeseh Ngwa et al., 2011; Asaithambi et al., 2014; Charli et al., 2016; Ponzoni et al., 2015). Morphological changes of the cells undergoing apoptosis after endosulfan treatment included shrunken cell bodies, cytoplasmic vacuolization, and membrane blebbing. For SYTOX green assay, SYTOX green dye enters only dead cells and binds with DNA to produce green fluorescence (Sherer et al., 2002). Briefly, cells grown in 24-well plates were treated with different concentrations of endosulfan for 20 h and then incubated with 1 μM SYTOX green for 20 min. Dead cells were viewed directly under the fluorescence microscope, as well as quantitatively measured using a fluorescence microplate reader (SpectraMax Gemini XS Model, Molecular Devices, Sunnyvale, California) with excitation at 485 nm and emission at 538 nm.

MTT assay. MTT (3-(4,5-dimethylthiazol-3-yl)-2,5-diphenyl tetrazolium bromide) assay was used to examine cell viability and determine the LC_{50} of endosulfan in N27 cells as described previously (Kitazawa et al., 2001; Latchoumycandane et al., 2004). Briefly, N27 cells (1×10^5 per well) were seeded in 24-well plates and incubated for 24 h. Then the medium was replaced with an endosulfan-containing medium with or without caspase inhibitors or autophagy inhibitor and the cells were further incubated for 15 h. After treatment, N27 cells were washed once and then incubated with 0.25 mg/ml MTT in serum-free medium for 3 h at 37°C. After that, the supernatant was removed and the formation of formazan (MTT metabolic product) was then solubilized in DMSO and further measured at 570 nm with a reference wavelength at 630 nm using a SpectraMax microplate reader.

MTS assay. Cell viability was measured using the Cell Titer 96® AQueous Non-Radioactive Cell Proliferation (MTS assay) kit from Promega as described previously (Charli et al., 2016; Jin et al., 2014). Briefly, N27 cells were plated at 1×10^5 cells/well in 96-well plates one day before treatment. The following day, medium was replaced with an endosulfan-containing medium with or without caspase inhibitors or autophagy inhibitor and the cells were further incubated for 15 h. Following treatment, 10 μl of MTS solution reagent mix was added to each plate well and incubated at 37°C for 45 min. At the end of incubation, the purple-colored formazan crystals that formed in the live cells were dissolved by adding 25 μl of DMSO to each well. Finally, readings were taken at a wavelength of 490 nm and another reference reading for each well was taken at 670 nm to eliminate background.

Western blot. After treatment, N27 cells were washed 3 times using PBS and then resuspended in homogenization buffer (pH 8.0, 20 mM Tris, 2 mM EDTA, 10 mM EGTA, 2 mM DTT, 1 mM PMSF, protease inhibitor cocktail) followed by sonication and centrifugation at 16 000 × g for 50 min at 4°C as described previously (Sarkar et al., 2017; Singh et al., 2018; Song et al., 2010). Cell lysates were resolved on 10%–15% SDS-PAGE and then transferred to nitrocellulose membranes for immunoblotting with different primary antibodies overnight, followed by secondary IR dye-800 conjugated anti-rabbit IgG or Alexa Fluor 680 conjugated anti-mouse IgG for 1 h at RT. Western blot was used to examine proteolytic activation of caspases and PKCδ, cytochrome c release into cytosol, LC3 protein level, Beclin-1 cleavage, and poly-ubiquitinated protein formation. Western blot images were captured with an Odyssey IR Imaging system (LI-COR) and data were analyzed using Odyssey 3.0 software.

Autophagic vacuole formation and MitoTracker or LysoTracker fluorescent staining. Following exposure to endosulfan at the time points 1, 3, or 6 h, N27 cells were examined under a phase-contrast microscope. Images were taken to show the autophagic vacuoles induced by endosulfan treatment. For visualization of mitochondria or lysosomes, live cells were incubated with 25 nM MitoTracker or LysoTracker (Invitrogen), respectively, for 10 min at 37°C before fixation. All images were analyzed by either C1 confocal microscopy (model TE-2000U; Nikon, Tokyo, Japan) or a SPOT digital camera and analyzed by MetaMorph software (Universal Imaging, Downingtown, Pennsylvania).

Transmission electron microscopy. For transmission electron microscopy (TEM), N27 cells on coverslips were fixed with 2% glutaraldehyde (w/v) and 2% paraformaldehyde (w/v) in 0.1 M sodium cacodylate buffer, pH 7.2, for 48 h at 4°C. Samples were washed in buffer and then fixed in 1% osmium tetroxide in 0.1 M cacodylate buffer for 1 h at RT. The samples were then dehydrated in 70% ethanol, contrast-stained with 2% uranyl acetate in 75% ethanol for 30 min, and further dehydrated in a graded ethanol series. They were then cleared with ultrapure acetone, infiltrated and embedded using a modified EPON epoxy resin (Embed 812; Electron Microscopy Sciences, Ft. Washington, Pennsylvania). Resin blocks were polymerized for 48 h at 70°C. Thick and ultrathin sections were made using a Leica UC6 ultramicrotome (Leeds Precision Instruments,

Minneapolis, Minnesota). Ultrathin sections were collected onto copper grids and imaged using a JEM 2100 200 kV scanning and transmission electron microscope (Japan Electron Optic Labs USA, Peabody, Massachusetts).

GFP-LC3 overexpression and puncta detection. N27 cells were transiently transfected with either the GFP-LC3 or GFP-LC3-ΔG plasmid using the Amaxa Nucleofector Kit (Lonza, Basel, Switzerland). Briefly, N27 cells were resuspended with the transfection buffer provided with the kit to a final concentration of 4–5 $\times$ 10^6 cells/100 μl and mixed with 5 μg plasmid DNA. Electroporation was executed with an Amaxa Nucleofector instrument following the manufacturer's protocol. Next, the transfected cells were plated at a density of 2.5 $\times$ 10^5 in 6-well plates for 24 h, treated with 60 μM endosulfan and then harvested at prespecified time points. Fluorescent microphotographs of GFP-LC3 were obtained from a SPOT digital camera and analyzed by MetaMorph software (Universal Imaging). The puncta staining of GFP-LC3 formed after endosulfan exposure, indicating the formation of autophagosomes.

Caspase enzymatic activity assay. Caspase enzymatic activities were assessed as described in our previous publications (Song *et al.*, 2010; Sun *et al.*, 2005). Following treatments, N27 cells were washed with PBS once, lysed with 10 μM digitonin in caspase assay buffer (50 mM Tris-HCl, 1 mM EDTA, 10 mM EGTA) at 37°C for 20 min, and then the lysates were centrifuged at 14 000 rpm. Next, aliquots of the cell-free supernatants were incubated in 96-well plates with different rows receiving 50 μM of a unique fluorogenic substrate, either Ac-VDVAD-AFC, Ac-DEVD-AFC, Ac-IETD-AFC, or Ac-LEHD-AFC for determination of caspase-2, -3, -8, or -9 activity, respectively. The formation of 7-amino-4-methylcoumarin (AFC), resulting from the caspase cleavage, was monitored at excitation 400 nm and emission 505 nm using a fluorescence plate reader (Molecular Devices). Caspase activities were normalized by protein concentration as measured by the Bradford method. Caspase-2 or caspase-3 proteolytic activation was also detected by Western blotting their respective antibodies.

Proteasome activity assay. The proteasomal peptidase assay was performed as described before (Song *et al.*, 2010; Sun *et al.*, 2005). Briefly, after endosulfan treatment, N27 cells were harvested, washed once in PBS and lysed in hypotonic buffer (10 mM HEPES, 5 mM $MgCl_2$, 10 mM KCl, 1% sucrose, and 0.1% CHAPS). Lysates then were incubated with a fluorogenic substrate Suc-LLVY-AMC (75 μM) in the proteasomal assay buffer (50 mM Tris-HCl, 20 mM KCl, 5 mM MgOAc, and 10 mM dithiothreitol, pH 7.6) at 37°C for 30 min. The cleaved fluorescent products (AMC) were then examined at the excitation and emission wavelengths of 380 and 460 nm, respectively, by a fluorescence plate reader (Gemini Plate Reader, Molecular Devices). Each lysate concentration was determined by the Bradford method and used to normalize enzymatic activity.

DNA fragmentation. DNA fragmentation assay was performed using a Cell Death Detection ELISA Plus Assay kit (Roche Diagnostics), as described in our recent publications (Sun *et al.*, 2005). This highly sensitive assay uses histone-associated low-molecular weight DNA found in the cytoplasm of cells. Briefly, after treatment, N27 cells were centrifuged, washed once with PBS and then incubated with cell lysis buffer (supplied with the kit) for 30 min at RT. After centrifuging, the supernatants were dispensed into streptavidin-coated 96-well microtiter plate wells containing 80 μl of HRP-conjugated antibody cocktail. After 2-h incubation at RT, the absorbance of the ELISA reaction was measured at 490 and 405 nm using a microplate reader (SpectraMax 190, Molecular Devices). The difference in absorbance between OD405 and OD490 nm was used to measure the actual DNA fragmentation level.

MDC assay. Monodansylcadaverine (MDC), an autofluorescent chemical, was used as a specific autophagolysosome marker to study autophagy in living cells. Incorporation of MDC into autophagic vacuoles induced by endosulfan treatment was measured by a fluorescence photometry plate reader (excitation wavelength 380 nm, emission filter 525 nm), as previously described (Munafo and Colombo, 2001). Briefly, following treatment with endosulfan, N27 cells were incubated with 50 μM MDC in PBS at 37°C for 20 min. Cells were then triple-washed with PBS and harvested in 10 mM Tris-HCl, pH 8, containing 0.2% Triton X-100. The intracellular MDC level was determined by fluorescence photometry. The number of cells present in each sample was detected by the measurement of DNA fluorescence (excitation 530 nm, emission 590 nm) by adding ethidium bromide to a final concentration of 0.2 mM and the value was used to normalize the MDC assay.

^{3}H-dopamine (^{3}H-DA) dopaminergic neurotoxicity assay. The effects of endosulfan on uptake of dopamine were assessed in fetal mouse mesencephalic cultures using ^{3}H-DA, as described in our recent publication (Song *et al.*, 2010). Briefly, after incubation for 20 h with 10, 20, 30, or 40 μM endosulfan, medium with the treatment was removed and cells were then washed once by assay incubation (Krebs-Ringer) buffer (5.6 mM glucose, 1.3 mM EDTA, 1.2 mM magnesium sulfate, 1.8 mM calcium chloride, 4.7 mM potassium chloride, 120 mM sodium chloride, and 16 mM sodium phosphate). Cells were incubated with 10 μM ^{3}H-DA (30 Ci/mol) for 20 min at 37°C. Negative controls were obtained by incubating the cells with 10 μM ^{3}H-DA together with 1 nM Mazindol (potent dopamine reuptake inhibitor). Uptake was stopped by removing the reaction mixture and triple-washing with fresh Krebs-Ringer buffer. Cells were then collected by using 1 N NaOH. Radioactivity was measured by liquid scintillation counting after adding a 5-ml scintillation cocktail to each vial.

Data analysis. Data analysis was performed using Prism 4.0 software (GraphPad Software, San Diego, California). Data were first analyzed using 1-way ANOVA and then Bonferroni's posttest was performed to compare all treatment groups. Differences with $p \leq .05$ were considered significant.

RESULTS

Endosulfan Is Cytotoxic to Dopaminergic Neuronal Cells

Although exposure to endosulfan has been shown to cause dopaminergic neurodegeneration and to deplete striatal dopamine levels in mice (Jia and Misra, 2007a,b), the cellular and molecular mechanisms of endosulfan-induced dopaminergic neuronal cell death remain unresolved. In this study, we first systematically examined endosulfan's acute effects during a 20-h, 20- to 80-μM exposure to establish its LC_{50} profile of dose-dependent neurotoxicity and cell death in our dopaminergic neuronal N27 cell line. Phase-contrast microscopy of endosulfan-treated cells revealed dose-dependent morphological changes indicative of apoptosis (Figure 1A). Dose-dependent cytotoxicity was also detected by SYTOX green fluorescence microscopy (Figure 1B).

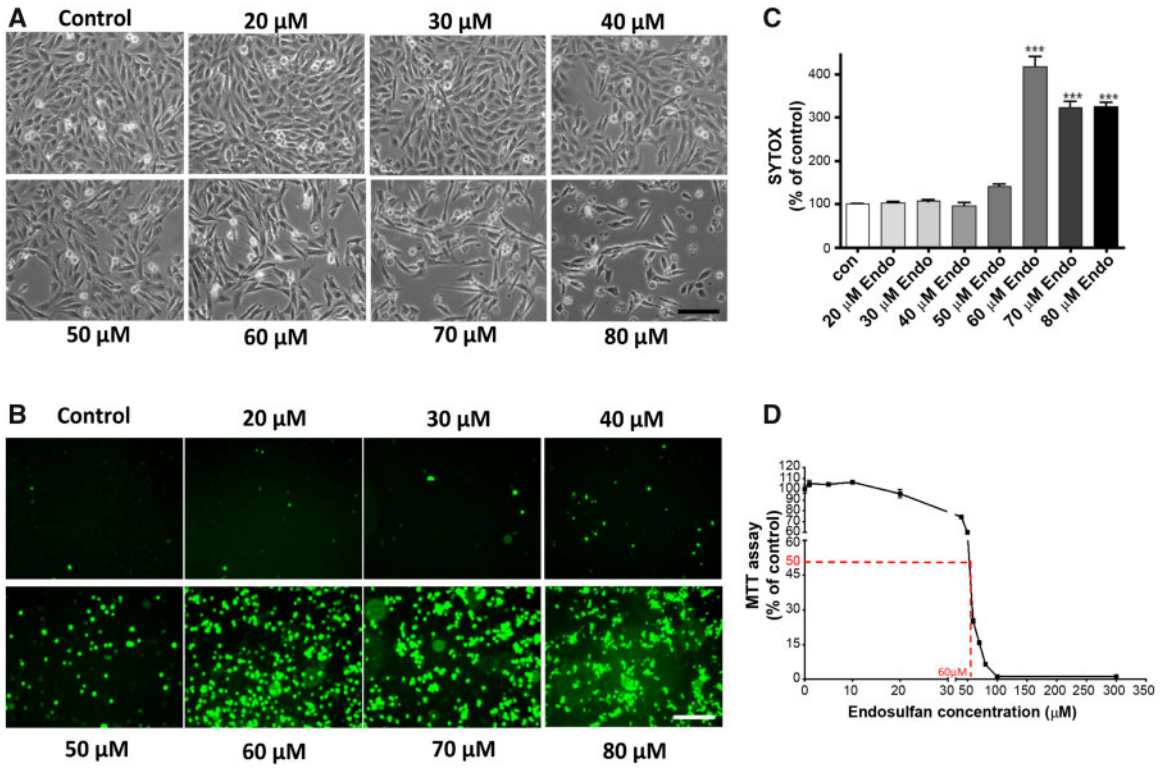

Figure 1. Endosulfan-induced cytotoxicity and cell death in dopaminergic neuronal N27 cells. N27 cells were treated with 20–80 μM endosulfan for 20 h. (A) Phase-contrast images of the cells treated with endosulfan, (B) SYTOX fluorescence staining in N27 cells treated with endosulfan, (C) SYTOX green fluorescence in cells treated with endosulfan was also quantified using a microplate reader. Scale bar, 100 μm. The data represent $n = 6$. ***, $p < .001$ represents significant differences between the endosulfan-treated group and the control cells treated with vehicle DMSO, and (D) endosulfan-induced apoptotic cell death as determined by MTT assay.

Quantification of SYTOX fluorescence (Figure 1C) revealed that 70 and 80 μM endosulfan elicited the most pronounced toxicity. Endosulfan's LC_{50} in N27 cells after a 20-h incubation was about 60 μM as determined by MTT assay (Figure 1D), and therefore 60 μM was used for further mechanistic studies.

Endosulfan Induces Autophagy in N27 Cells

During endosulfan treatments, we inspected the formation of autophagic vacuoles that were visible as early as 1 h post-treatment. The size and number of vacuoles progressively increased with the exposure duration of 60-μM endosulfan treatment increased (up to 6 h), compared with vehicle control cells treated with DMSO (Figure 2A, arrows in top panel). To better simulate the physiological concentrations of endosulfan that people might be exposed to in the environment, we used low concentrations of endosulfan (10–30 μM) for a long-term exposure to further examine the formation of autophagic vacuoles. Similarly, low-concentration endosulfan also increased vacuole formation (Figure 2A, lower panel). Because these vacuoles resemble the double-membrane autophagic vacuoles (autophagosomes and autolysosomes) that sequester bulk cytoplasmic contents (Gozuacik and Kimchi, 2004), we then tested via LysoTracker staining whether the vacuoles formed at a late time point contained lysosomes and if some of them contained defective cytoplasmic contents, such as mitochondria, using MitoTracker staining. After a 9-h endosulfan treatment, some vacuoles were empty (Figure 2B, indicated by arrow) and some of them contained mitochondria (indicated by *). LysoTracker labeling suggested that some of the autophagosomes can merge with lysosomes to form autolysosomes (indicated by open arrows). To further examine whether endosulfan induces autophagy, we investigated the ultrastructure of N27 cells with and without endosulfan treatment by TEM. We observed numerous vacuolar elements that assembled autophagic vacuoles in endosulfan-treated cells (Figure 2C).

To confirm that the formed vacuoles induced by endosulfan were autophagosomes, we used the reliable autophagy marker LC3, the first mammalian protein found to localize with autophagosomes during autophagy. Thus, the formation of autophagosome puncta containing LC3 has been regarded as a hallmark of autophagic activation. For this, N27 cells were transiently transfected with GFP-LC3 plasmids and then treated with endosulfan. We then traced the redistribution of LC3 during the formation of autophagosomes at different time points under fluorescence microscopy (Figure 2D). In control cells, GFP-LC3 green fluorescence was diffusely distributed in the cytoplasm. In contrast, in endosulfan-treated cells, characteristic puncta (fluorescent dots) formed in a time-dependent manner. It has been reported that spontaneous lipid independent aggregation of GFP-LC3 occurs when it is overexpressed in cells (Tanida *et al.*, 2008). To identify lipidation-independent LC3 puncta, we used a negative plasmid control, GFP-LC3-ΔG, in which the C-terminal glycine essential for lipidation has been deleted. Endosulfan treatment did not induce fluorescent puncta formation in GFP-LC3-ΔG-transfected cells, indicating that the puncta dots formed in GFP-LC3-transfected cells are lipid-associated (Figure 2D).

Of the two isoforms of LC3, the cytoplasmic form, LC3-I, can be proteolysed at a specific site producing LC3-II, which is associated with membrane compartments, such as autophagosomes during autophagy (Kabeya *et al.*, 2000; Sy *et al.*, 2008).

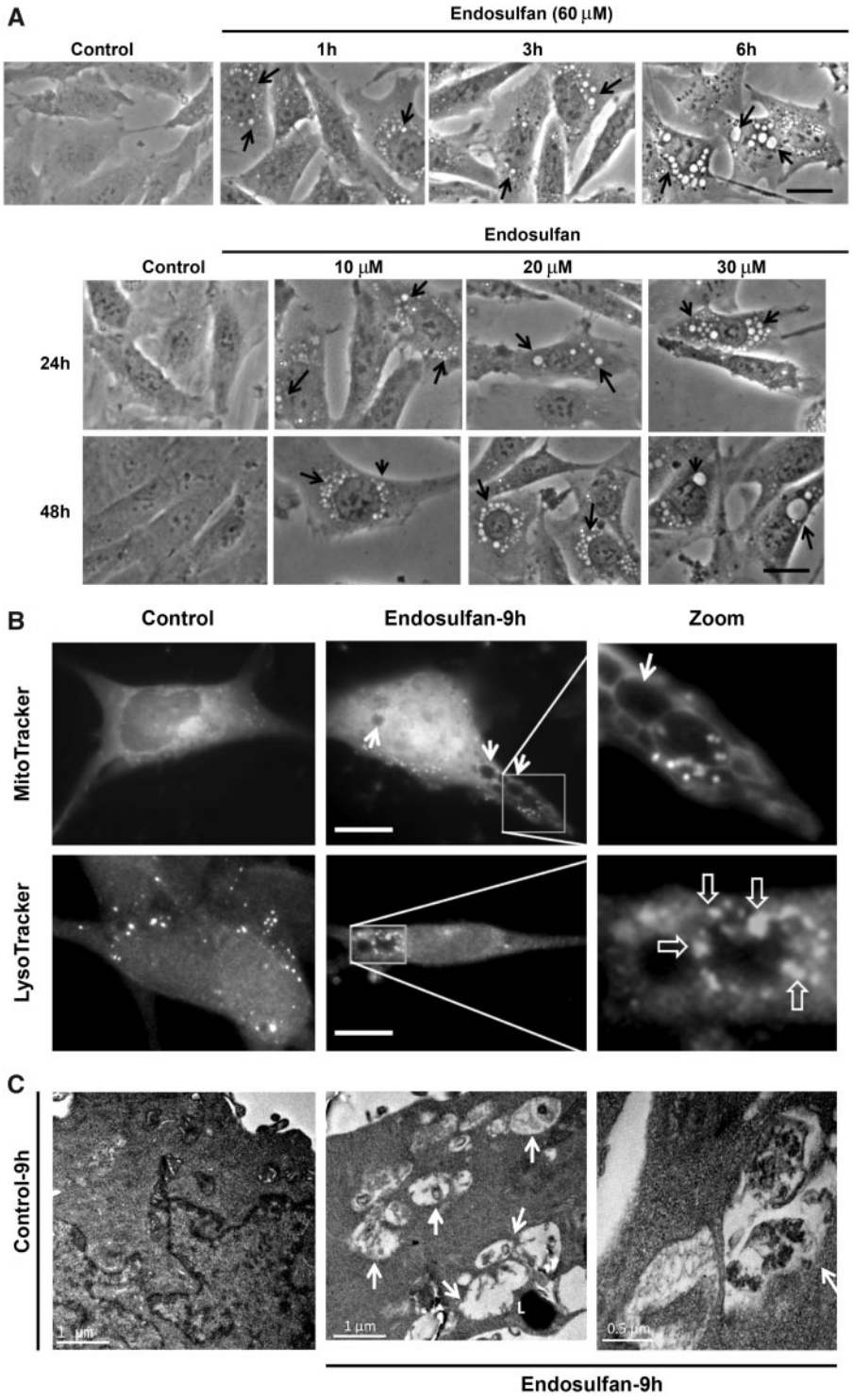

Figure 2. Endosulfan-induced autophagy in N27 dopaminergic neuronal cells. (A) Autophagic vacuoles were examined by phase-contrast microscopy. Scale bar, 10 μm. (B) MitoTracker and LysoTracker fluorescent staining imaged after 9-h exposure to endosulfan. Scale bar, 10 μm. (C) Representative transmission electron microscopy images depicting the ultrastructure of cells treated with 60 μM endosulfan for 9 h. *Arrows*, autophagic vacuoles. *Arrowheads*, autophagosome assembly (cargo capturing). Scale bars 0.5 and 1 μm. (D) Cells were transfected with one of the GFP-LC3 fusion constructs (wild type or mutant ΔG). Puncta formed in cells transfected with GFP-LC3 cDNA and treated by endosulfan for 3 and 6 h. GFP-LC3 dots were not observed when cells were transfected with GFP-LC3-ΔG cDNA. Scale bar, 10 μm. (E) Immunoblot analyses of accumulating LC3-II protein in cells treated with 60 μM endosulfan; β-actin expression was used as an equal loading control. (F) MDC assay was performed in control or endosulfan-exposed cells. ***, $p < .001$ indicates significant differences between endosulfan-treated groups and vehicle-treated control cells.

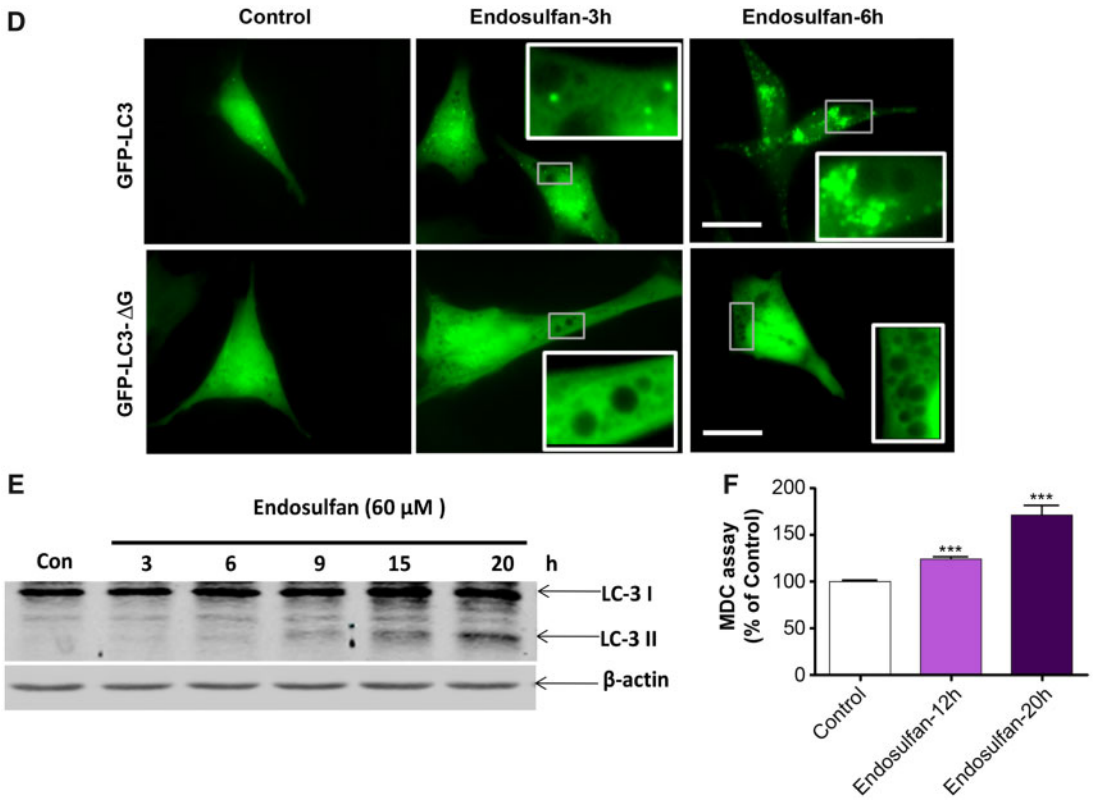

Figure 2. Contined

Generally, LC3-II protein levels increase with enhanced autophagosome formation. In our study, LC3-II steadily increased in endosulfan-treated cells as revealed by Western blot (Figure 2E).

Finally, because the autofluorescent drug MDC has been recognized as a specific marker for autophagosomes (Biederbick *et al.*, 1995), we performed an MDC assay to confirm endosulfan-induced autophagy as measured by the buildup of MDC fluorescence in cells. To increase the assay signal, we chose 12 and 20 h (late phase after autophagy) post endosulfan treatment to accumulate the autofluorescent drug MDC. MDC accumulated time-dependently during endosulfan (60 μM) treatment (Figure 2F). Collectively, our results clearly demonstrate that endosulfan induces an autophagic response in a dopaminergic neuronal model.

Endosulfan Inhibits Proteasomal Activity and Induces Aggregation of High-Molecular Weight (HMW) ubiquitinated Proteins in Dopaminergic Neuronal Cells

The findings of an endosulfan-induced autophagic response prompted us to further investigate the cause of autophagy. The ubiquitin proteasome system (UPS) and autophagy machinery are the two major degradation systems in the cell and the UPS is suspected of playing a role in the pathogenesis of PD (Biasini *et al.*, 2003; Dantuma and Bott, 2014; Martins-Branco *et al.*, 2012; Sun *et al.*, 2005, 2006). Proteasome inhibition could activate autophagy to compensate for the proteasome degradation system (Ding *et al.*, 2007). Our previous studies showed that another organochlorine pesticide, dieldrin, caused a significant impairment of the proteasomal machinery and neurodegeneration of dopaminergic cells (Song *et al.*, 2010; Sun *et al.*, 2005). Therefore, we examined the effect of endosulfan exposure on proteasomal activity in N27 dopaminergic neuronal cells. N27 cells exposed to 0–80 μM endosulfan for 20 h showed a dose-dependent reduction in proteasomal activity (Figure 3A). Because the EC_{50} of endosulfan for N27 cells was 60 μM (see Figure 1D), we then conducted a time-course analysis of proteasomal activity with 60-μM endosulfan exposure at earlier time points. Proteasomal activity decreased significantly within 3 h after endosulfan treatment and remained roughly constant during the entire treatment period (Figure 3B). As reported previously, due to the decreased rate of protein clearance by the proteasome, UPS dysfunction can result in the accumulation of ubiquitinated proteins in the cytosol (Rideout and Stefanis, 2002). As further confirmation of UPS impairment, endosulfan treatment led to a dramatic accumulation of HMW ubiquitin-conjugated proteins in cells after 3 h, as revealed by Western blot (Figure 3C). These results suggest that endosulfan treatment causes the accumulation of HMW ubiquitin-conjugated proteins by rapidly impairing the UPS.

Prolonged Exposure to Endosulfan Induces Apoptotic Cell Death

After prolonged endosulfan treatment, we observed an apoptosis-like cell death in N27 dopaminergic neuronal cells. Previous reports indicate that endosulfan decreases cell growth and causes apoptosis in germ cells, blood mononuclear cells, neuroblastoma cells and neural stem cells (Ahmed *et al.*, 2008; Jia and Misra, 2007b; Kang *et al.*, 2001; Ren *et al.*, 2008). We have previously demonstrated caspases-3 and 9 and proteolytic activation of PKCδ mediate dieldrin-induced apoptotic cell death (Kitazawa *et al.*, 2004). Recently, caspase-2 has been suggested to play critical roles in stress-induced apoptotic cell death and

cell-cycle maintenance (Bouchier-Hayes, 2010). As reported, pro-caspase-2 can be cleaved into several fragments (32–33, 14, 18, and 12 kDa), and 18/12 kDa are the active subunits (Li *et al.*, 1997). Thus, we examined whether endosulfan-induced cell death in dopaminergic neuronal N27 cells results from apoptosis. We treated cells with 60 μM endosulfan for 6, 9, 15, and 20 h. Although the executioner caspase-3 was significantly activated after the 9-h treatment, accompanied by activation of caspase-2, the mitochondria-initiated apoptotic events, such as cytochrome c release and activation of the initiator caspases 8 and 9, were not evident until the 15-h treatment (Figs. 4A and 4B). In addition to caspase enzymatic activation, we also demonstrated the proteolytic cleavage of caspase-2 and -3 by Western blot (Figs. 4C and 4D). Previously, we demonstrated that many neurotoxins induce apoptotic cell death by caspase-3-dependent proteolytic activation of protein kinase C delta (PKCδ) (Kaul *et al.*, 2003; Kitazawa *et al.*, 2003; Latchoumycandane *et al.*, 2004), which we routinely use as another apoptotic marker. Exposure to 60 μM endosulfan over a 15- or 20-h time period resulted in the proteolytic cleavage of native PKCδ (78 kDa) into cleaved fragments forming 38- and 41-kDa bands (Figure 4E).

DNA fragmentation has been noted during apoptotic cell death and considered as a key marker of apoptosis. Therefore, to determine if endosulfan induces DNA fragmentation, we treated N27 cells with 60 μM endosulfan for 6, 9, 15, and 20 h. After the 9-h treatment, DNA was significantly fragmented compared with the control (Figure 4F) as examined by an ELISA sandwich assay described in our previous publications (Kaul *et al.*, 2005; Sun *et al.*, 2008).

These results show that endosulfan treatment eventually leads to apoptosis through caspase activation, cytochrome c release, PKCδ proteolytic activation, and DNA fragmentation. It is also noteworthy that endosulfan-induced apoptosis might be considered as a late event (starting at 9 h in Figure 4), triggered by a cascade of preceding autophagic responses to endosulfan treatment, including autophagic vacuole formation, GFP-LC3 recruitment and puncta formation, and elevated LC3-II (Figure 2).

Multiple Caspases Mediate Endosulfan-Induced PKCδ Cleavage and Apoptotic Cell Death

Because we noticed caspase-2 and -3 activities were dramatically activated before caspase-8 and -9 activation and mitochondrial cytochrome c release, we then investigated whether caspase-2 and -3 activation works as an upstream event before caspase-8 and -9 activation. We found that 60 μM endosulfan significantly increased both caspase-8 and -9 activity after 20 h, whereas co-treatment with 50 μM of the specific inhibitor for caspase-2 (Z-VDVAD-fmk) or caspase-3 (Z-DEVD-fmk) completely blocked endosulfan-induced caspase-8 and -9 activation (Figs. 5A and 5B), as examined by caspase enzymatic activity using caspase-8 or -9 specific substrates. To further determine the effect of caspase-2 or caspase-3 inhibition on endosulfan-induced cell death, we used the SYTOX green cytotoxicity and MTT assays. Quantification of both assays revealed significant protection against endosulfan-induced neurotoxicity by caspase-2 or -3 inhibition (Figs. 5C and 5D). Previously, we and others have shown that PKCδ is a well-known downstream substrate of caspases and its proteolytic cleavage is actively involved in cell apoptosis (Emoto *et al.*, 1995; Kanthasamy *et al.*, 2003, 2006; Kitazawa *et al.*, 2003). We then used PKCδ as a marker to reveal apoptotic cell death processes. Exposure to 60 μM endosulfan caused phosphorylation of PKCδ at Threonine 505 (T505) (Figure 5E). Knockout of PKCδ by CRISPR/Cas9 significantly reduced endosulfan-induced phosphorylation of PKCδ, proteolytic cleavage of caspase-3 (Figure 5F), and neuronal cytotoxicity (Figure 5G). Furthermore, endosulfan exposure induced proteolytic cleavage of PKCδ evident at later time points (15 and 20 h), whereas co-treatment with 50 μM of a caspase-2 or -3 specific inhibitor significantly attenuated endosulfan-induced PKCδ proteolytic cleavage (both 15 and 20 h) (Figs. 5H and 5I). The CRISPR/Cas9 PKCδ knockdown efficiency was shown to be about 85% (Supplementary Figure 1). Compared with caspase-3 inhibition, caspase-2-specific inhibition was more effective and almost completely blocked endosulfan-induced PKCδ cleavage.

Growing evidence suggests that PKCδ can play a dual role, either promoting or suppressing autophagy, depending on the cell type involved and the stimulus used to induced autophagy (Chen *et al.*, 2009; Zhang *et al.*, 2017a). To further characterize the role of PKCδ in endosulfan-induced autophagy, we used a CRISPR/Cas system to genetically knock down endogenous PKCδ levels. Transduction of N27 cells with the CRISPR/Cas9-based PKCδ KD lentivirus dramatically inhibited the endosulfan-induced conversion of LC3-I to LC3-II (Figure 5E). Also, knocking down PKCδ minimized the cleavage of caspase 3 and PKCδ phosphorylation activation (Figure 5E), suggesting a positive feedback activation of caspase-3 by PKCδ. These results suggest that caspase inhibitors attenuate endosulfan-induced cytotoxicity and apoptotic cell death and that PKCδ plays a role in the crosstalk between endosulfan-induced autophagy and apoptosis.

Autophagy Inhibitors Potentiate Endosulfan-Mediated Apoptotic Cell Death

The interconnection between endosulfan-induced autophagy and apoptosis was further explored using the autophagy inhibitor wortmannin or bafilomycin A1. Wortmannin is an inhibitor of phosphatidylinositol 3-kinase (PI3K), which is required for autophagy (Blommaart *et al.*, 1997). Therefore, wortmannin exerts an autophagy-inhibiting effect and blocks autophagy at an early stage prior to autophagosome formation (Blommaart *et al.*, 1997; Munafo and Colombo, 2001; Yu *et al.*, 2006). Bafilomycin A1 inhibits autophagy by blocking the maturation of autophagic vacuoles at the phase of fusion between autophagosomes and lysosomes (Klionsky *et al.*, 2008; Redmann *et al.*, 2017; Shacka *et al.*, 2006). Treatment of N27 dopaminergic neuronal cells with wortmannin effectively blocked the formation of autophagosomes and the GFP-LC3 fluorescent puncta induced by endosulfan (Figure 6A). Bafilomycin A1 co-treatment significantly decreased endosulfan-induced LC3 II formation (Figure 6B). Wortmannin at 50 nM was nontoxic to the cells, however, after a 6-h treatment, endosulfan led to significant increases of caspase-2 and -3 activity in the presence of wortmannin or bafilomycin A1 (Figs. 6C–F), whereas cells exposed to either compound alone for 6 h did not (Supplementary Figure 2). Cytotoxicity and cell death were also exacerbated when cells were exposed to endosulfan in the presence of wortmannin or bafilomycin A1 as demonstrated in the SYTOX green and MTS assays (Figs. 6G–J). Collectively, these results indicate that wortmannin or bafilomycin A1 inhibited endosulfan-mediated autophagy and rendered the cells more sensitive to the cytotoxic actions of endosulfan through the initiation of apoptosis.

Beclin-1 Is Involved in Endosulfan-Induced Autophagy and Apoptosis

As demonstrated thus far, autophagy and apoptosis can be sequentially triggered by endosulfan with autophagy serving as a pro-survival process against endosulfan-induced cell death.

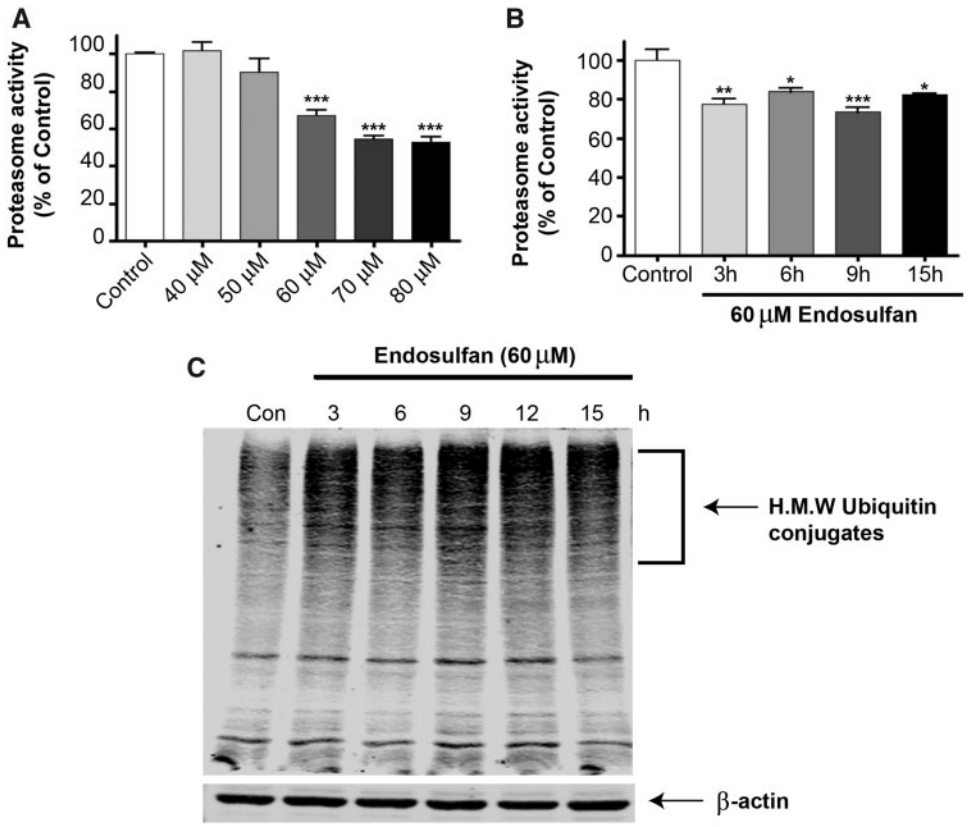

Figure 3. Endosulfan inhibited proteasomal activity and triggered HMW ubiquitinated protein aggregation in N27 cells. (A) N27 cells were exposed to various concentrations of endosulfan ranging from 40 to 80 μM for 20 h. (B) Cells were exposed to 60 μM endosulfan for 3–15 h. Chymotrypsin-like proteasome activity was measured using the fluorogenic substrate Suc-LLVY-AMC (75 μM). Asterisks (***, $p < 0.001$) indicate statistically significant differences compared with vehicle-treated control cells. (C) Accumulation of HMW ubiquitin-conjugated protein in N27 cells exposed to 60 μM endosulfan. Equal amounts of proteins were resolved on 10% SDS poly-acrylamide gel electrophoresis and blotted with ubiquitin antibody.

However, the actual event initiating the switch from autophagy to apoptosis remains unclear. Bcl-2-interacting protein-1 (Beclin-1), the mammalian homolog of yeast autophagic gene Atg6, is a component of the class III PI3K complex crucial for autophagosome formation and a key factor in autophagy signaling (Kihara *et al.*, 2001; Liang *et al.*, 1999). The latest studies demonstrate that a caspase-mediated cleavage of Beclin-1 not only abolishes its autophagic function but also accelerates the apoptotic pathway (Cho *et al.*, 2009; Djavaheri-Mergny *et al.*, 2010; Wirawan *et al.*, 2010). Thus, we investigated whether Beclin-1 cleavage also occurs during endosulfan-caused cell death. After prolonged endosulfan treatment (15 h), a 37-kDa cleaved fragment of Beclin-1 was observed and this band accumulated with time (Figure 7A). To explore whether Beclin-1 cleavage in the present study was mediated by caspases, Beclin-1 cleavage was examined after blocking caspases. Inhibition via the caspase-2 inhibitor Z-VDVAD-fmk or the caspse-3 inhibitor Z-DEVD-fmk effectively diminished the cleavage of Beclin-1 (Figure 7B), thereby confirming the involvement of caspases in Beclin-1 cleavage. The ability of caspase inhibitors to attenuate the Beclin-1 cleaved band at 37 kDa also confirmed that the 37-kDa band is not a nonspecific background band, but a real cleaved fragment of Beclin-1. It was also notable that the caspase-2 inhibitor was more effective than the caspase-3 inhibitor and almost totally blocked Beclin-1 cleavage. These results collectively demonstrate that Beclin-1 was proteolytically cleaved by caspases after our prolonged endosulfan treatments and this cleavage might play a critical role in the crosstalk between autophagy and apoptosis. Studies are underway to identify the real function of Beclin-1 cleavage and the cell signaling cascades that follow.

Endosulfan Induces Autophagy and Dopaminergic Neuronal Cell Loss in Primary Neuronal Cultures

We further assessed the effect of endosulfan on nigrostriatal dopaminergic neurons using primary neuronal cultures. Mouse primary dopaminergic neuronal cultures were treated with 40 μM endosulfan, and then the formation of autophagic vacuoles was examined by phase-contrast microscopy of striatal (STR) neurons or by TH immunostaining specifically for dopaminergic neurons. Endosulfan induced the formation of autophagic vacuoles in both striatal and nigral neurons (Figs. 8A and 8B, arrows). We further confirmed autophagy by showing a steady increase in LC3-II formation in endosulfan-treated primary cultures as revealed by Western blot (Figure 8C). The effects of endosulfan neurotoxicity on dopaminergic neuronal function were assessed by dopamine uptake assay. The 20-h endosulfan treatment significantly decreased both dopamine uptake and the number of TH^+ neurons, indicating TH^+ neuronal degeneration (Figure 8D). Together, these results demonstrate that the neurotoxicant endosulfan can induce autophagy and neuronal cell degeneration in nigrostriatal dopaminergic neurons.

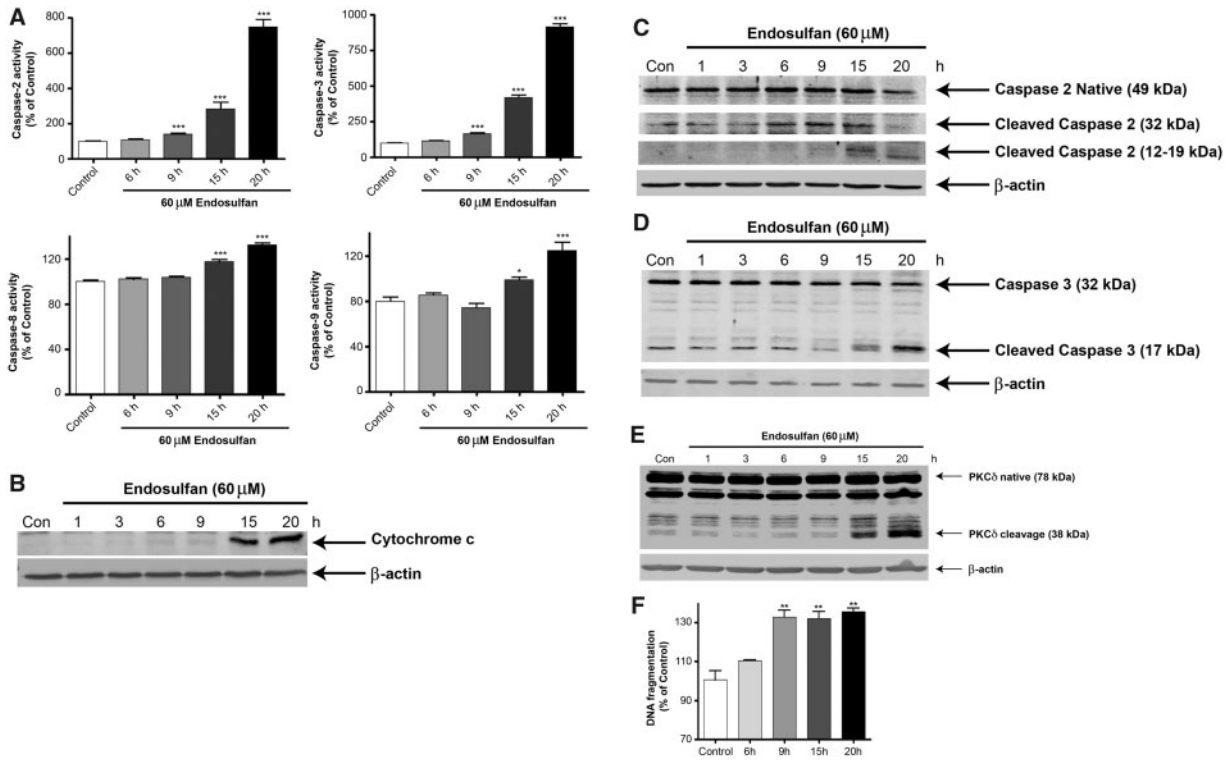

Figure 4. Endosulfan treatment increased apoptotic cell death in N27 cells. N27 cells were exposed to 60 μM endosulfan for 6, 9, 15 or 20 h. (A) Caspase-2, -3, -8, or -9 enzymatic activities were measured by their specific fluorogenic caspase substrates. Asterisks (*, $p < .05$, ***, $p < .001$) indicate significant differences between endosulfan-treated groups and vehicle-treated control cells. Western blots after endosulfan treatment showing (B) the release of cytochrome c into the cytoplasm from mitochondria, (C) caspase-2 activation measured by cleaved caspase-2, (D) caspase-3 proteolytic activation, and (E) PKCδ cleavage. Equal loading of protein was demonstrated using β-actin. (F) Apoptotic cell death was determined by measuring DNA fragmentation in an ELISA sandwich assay. **, $p < .01$ indicates significant difference between endosulfan-treated cells and vehicle DMSO-treated control cells.

DISCUSSION

A definitive role for autophagy in cell survival and cell death remains controversial (Galluzzi *et al.*, 2008; Levine and Yuan, 2005), with reports suggesting autophagy either promotes or counteracts cell death, depending on cell type, cellular circumstances, and stimuli (Boya *et al.*, 2005; Scott *et al.*, 2007; Yu *et al.*, 2006). In the present study, we report that the organochlorine pesticide endosulfan induced autophagy followed by apoptotic cell death and we verify that autophagy played an early pro-survival role during this process. We first observed the presence of autophagic hallmarks, including an increased number of autophagosomes, an accumulation of LC3-II, and an increased uptake of MDC in an endosulfan-exposed N27 dopaminergic neuronal model. Then, distinctive apoptotic symptoms, including caspase activation, cytochrome c release, PKCδ proteolytic activation and DNA fragmentation appeared after prolonged endosulfan treatment. Moreover, we show that caspase-2 or -3 inhibitors retarded apoptosis but not autophagy, which suggests that apoptosis was induced via a caspase-dependent pathway and autophagy occurred as an upstream event preceding apoptotic cell death. Further investigation revealed that CRISPR/Cas9-based stable knockdown of PKCδ in N27 dopaminergic cells reduced the levels of endosulfan-induced caspase-3, suggesting a PKCδ-dependent regulatory mechanism involved in endosulfan-induced apoptosis. Additionally, the inhibition of autophagy by wortmannin significantly enhanced apoptotic signaling, cytotoxicity, and cell death in endosulfan-treated dopaminergic neuronal N27 cells, suggesting an upstream protective role of autophagy. Finally, we show that endosulfan exposure led to autophagy induction and neurodegeneration in nigrostriatal dopaminergic primary cultures.

Although the signal cascades and molecular mechanisms activating autophagy are not yet fully understood, it has been demonstrated that UPS dysfunction might be a trigger for stimuli-induced autophagy (Li *et al.*, 2010; Matsuda and Tanaka, 2010; Pan *et al.*, 2009; Zheng *et al.*, 2009). As shown in Figure 3, endosulfan exposure impaired the UPS, resulting in the accumulation of ubiquitinated proteins. Therefore, we hypothesize that during the early stages of endosulfan treatment, UPS dysfunction can stimulate autophagy to serve as a compensatory pathway to degrade cytosolic components or impaired proteins. But during prolonged endosulfan exposures, the autophagy machinery becomes overburdened and then apoptotic cell death ensues. Under this hypothesis, autophagy works as a compensatory protective mechanism, retarding the occurrence of apoptosis. This notion is supported by our findings that the inhibition of autophagy by wortmannin rendered N27 cells more sensitive to endosulfan-induced cytotoxicity and apoptotic cell death.

Neurotoxic stress-induced apoptosis is a mitochondria-dependent pathway, wherein the release of cytochrome c into the cytosol is regarded as the signal that initiates the onset of apoptosis. Released cytochrome c then activates caspase-9, which further proteolytically cleaves the “executioner” caspase-3 and mediates irreversible apoptotic cell death (Green and Reed, 1998; Kroemer and Reed, 2000; Robertson and Orrenius, 2000; Sy *et al.*, 2008; Wilson, 1998). Our results indicate that

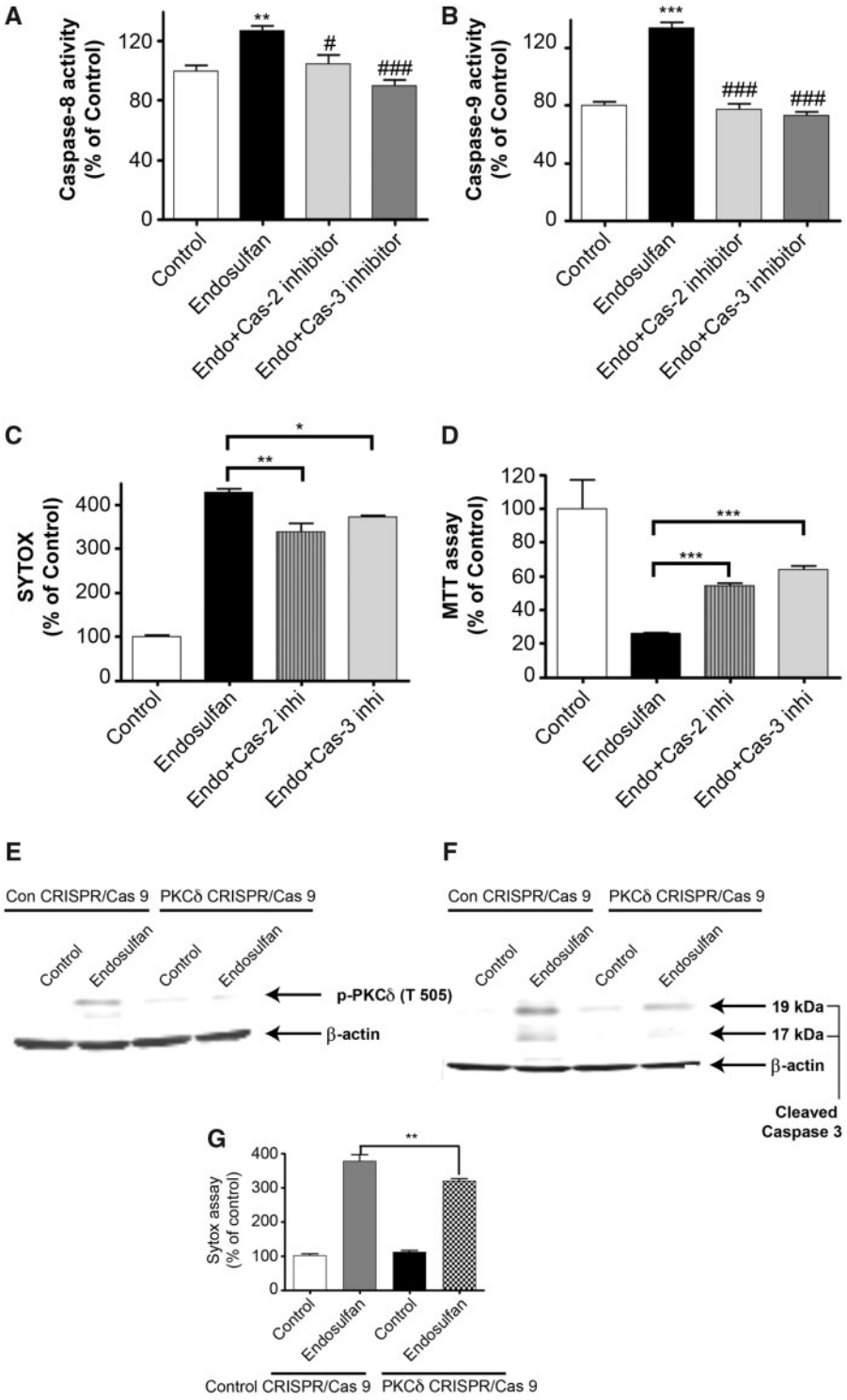

Figure 5. Caspase-2 or -3 inhibition attenuated endosulfan-induced apoptosis but did not affect the autophagy process in N27 cells. N27 cells were pretreated with 50 μM of inhibitor of caspase-2 (Z-VDVAD-fmk) or caspase-3 (Z-DEVD-fmk) for 1 h and then exposed to 60 μM endosulfan. (A, B) Caspase-2 and caspase-3 inhibitors attenuated endosulfan-induced activation of caspase-8 and -9. Hashtags (#$p<.05$; ###$p<.001$), between Endosulfan+caspase inhibitor and Endosulfan. (C) SYTOX green fluorescence in cells after 15-h treatment. (D) Cell viability was assayed using MTT. (E, F) PKCδ T505 phosphorylation and caspase-3 cleavage were detected by Western blots of control CRISPR/Cas9 and PKCδ CRISPR/Cas9-knockdown N27 cells treated with or without 60 μM endosulfan for 20 h. (G) SYTOX assay demonstrates that PKCδ knockdown attenuated endosulfan-induced neurotoxicity as compared with control cells. (H) PKCδ cleavage was measured after 9, 15, or 20 h by immunoblotting cell lysates. (I) Quantification of the PKCδ cleavage immunoblot. The data represent $n = 6$. Asterisks (*$p < .05$; **$p < .01$; ***$p < .001$).

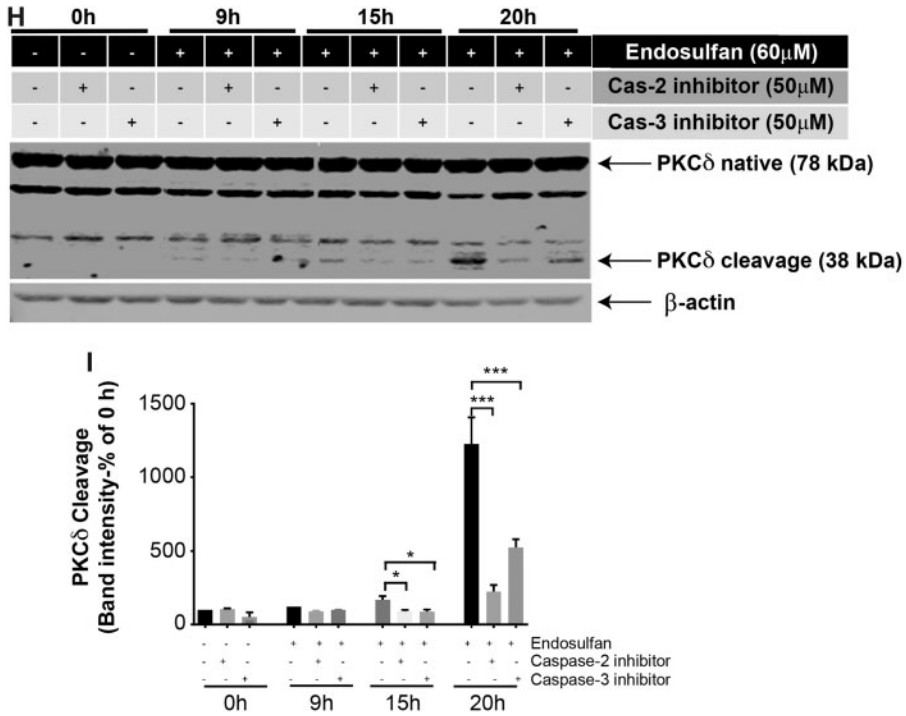

Figure 5. Continued.

proteolytic activation of caspase-2 and -3 occurs before cytochrome c release and activation of initiator caspase-8 or -9. We propose that another signal transduction pathway must activate caspase-2 or -3, acting upstream of the mitochondria-dependent pathway. Based on their structure and function, caspases basically can be classified into two groups: initiator caspases (caspase-2, -8, -9, and -10) or executioner caspases (caspase-3, -6, and -7). Initiator caspases have adapter domains on their N-termini, allowing their autocleavage and downstream caspase activation, whereas executioner caspases do not contain such adaptor domains so that they can only be cleaved and activated by initiator caspases (Kuribayashi *et al.*, 2006). Initiator caspase-8 and -10 are the apical caspases reported to initiate death-receptor-mediated apoptosis. Initiator caspase-9 is activated by cytochrome c release and involved in the mitochondria-dependent apoptotic pathway. A number of recent studies demonstrate that caspase-2, as an initiator caspase, acts before mitochondrial damage and promotes cytochrome c release and apoptosis (Harvey *et al.*, 1997; Krumschnabel *et al.*, 2009; Lin *et al.*, 2004; Read *et al.*, 2002). Therefore, our present findings, showing that caspase-2 acts as the upstream initiator of caspase-8 and the mitochondria pathway-related initiator caspase-9, suggest that caspase-2 works as a central initiator caspase to activate caspase-3 and magnify apoptosis in endosulfan-mediated cell death, independent of mitochondrial apoptosis.

The molecular factors involved in the crosstalk of autophagy and apoptosis have already been reported to be critical in determining cell survival or death (Chen *et al.*, 2009; Cheng *et al.*, 2008; Cho *et al.*, 2009; Djavaheri-Mergny *et al.*, 2010; Luo and Rubinsztein, 2010). Beclin-1 (Atg6), part of the class III PI3K complex, is an essential autophagy initiator (Furuya *et al.*, 2005; Levine and Deretic, 2007; Maiuri *et al.*, 2010). Previous reports indicate that Beclin-1 can be cleaved by caspases, and after cleavage, Beclin-1 lacks pro-autophagic ability but gains a new function to facilitate apoptosis through a mitochondrion-dependent pathway (Cho *et al.*, 2009; Djavaheri-Mergny *et al.*, 2010; Wirawan *et al.*, 2010). In our present study, we also found that after prolonged endosulfan treatment, Beclin-1 exhibits caspase-mediated cleavage. More interestingly, caspase-2 inhibition can also block Beclin-1 cleavage even more effectively than does caspase-3 inhibition, which was a novel finding from this study. Thus, we propose that caspase-2 is the upstream initiator caspase and caspase-3 is the downstream executioner caspase in endosulfan-mediated Beclin-1 cleavage. Interestingly, treatment with inhibitors for caspase-2 and caspase-3 induced a subtle Beclin-1 cleavage in control cells (no endosulfan treatment) (Figure 7B). As reported, Beclin-1 can be cleaved by caspase-3, -7, -8, and calpain; therefore, it is possible that other proteases were activated when caspase-2 or -3 was inhibited (Cho *et al.*, 2009; Luo and Rubinsztein, 2010). Being involved in both autophagy and apoptosis, Beclin-1 seems to become a key factor in endosulfan-mediated cell death. Therefore, it will be worthwhile to investigate the downstream signaling events after Beclin-1 cleavage to explore the mechanisms of apoptosis. We believe that a noncleavable Beclin-1 mutant would be helpful in testing if restoring autophagy retards neurotoxin-mediated apoptotic cell death. Studies are underway to identify the cleaved site of Beclin-1 and to clarify the role of this cleavage induced by prolonged exposure to endosulfan. Furthermore, to better establish toxicological relevance, we developed a heuristic model of the adverse outcome pathway. This AOP highlights the order of molecular events and the cellular key events involved in the degeneration of dopaminergic neuronal cells exposed to endosulfan (Figure 9).

In summary, we present a novel finding that the environmental neurotoxicant endosulfan induces autophagy as an

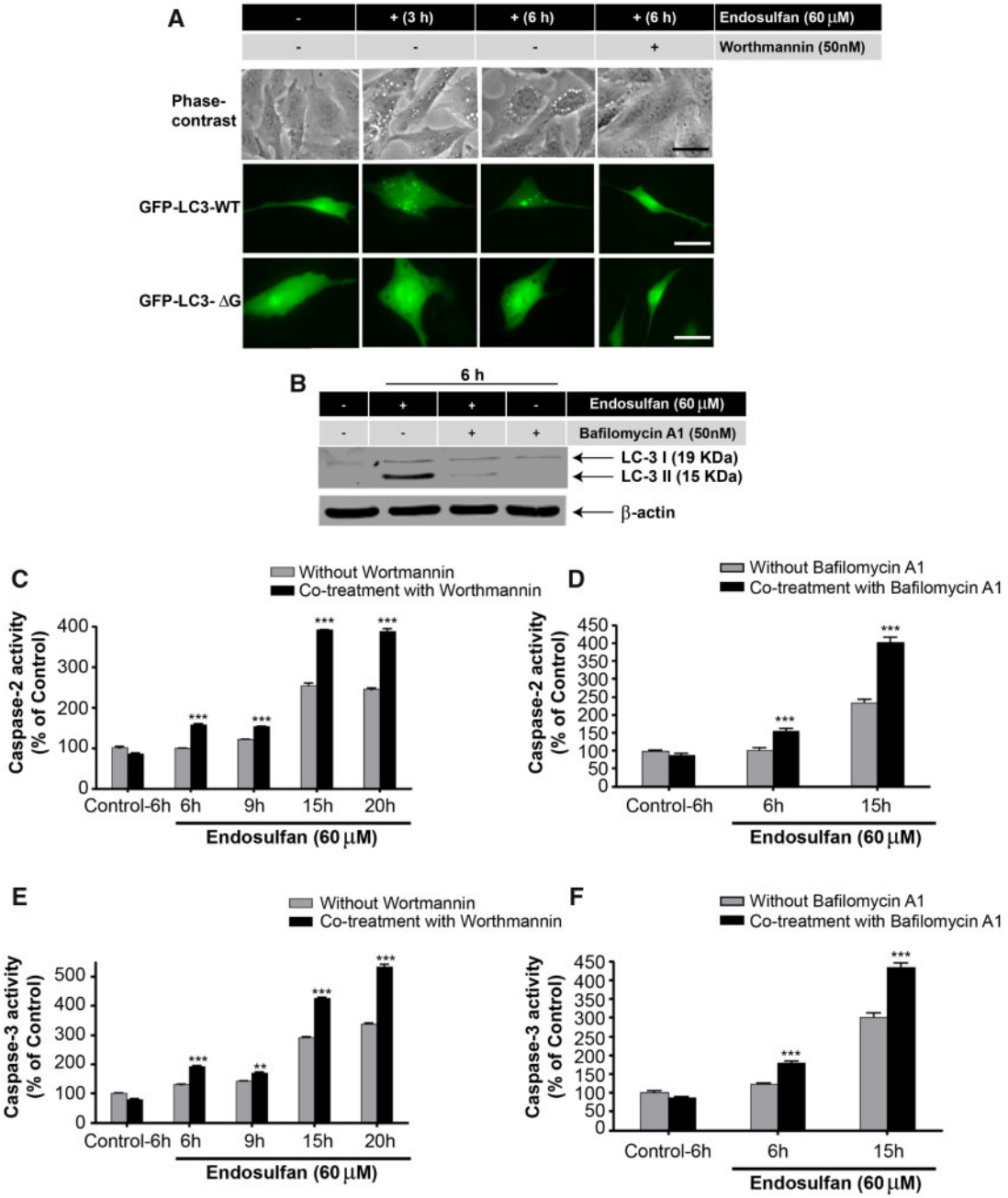

Figure 6. Inhibition of autophagy by wortmannin or bafilomycin A1 makes N27 cells more sensitive to endosulfan-induced apoptotic cell death. N27 cells were exposed to endosulfan with or without 50 nM of the autophagy inhibitor wortmannin. (A) Endosulfan-caused autophagosome formation with or without wortmannin co-treatment examined by phase-contrast microscopy or by fluorescence microscopy of puncta formation of GFP-LC3. Scale bar, 10 μm. (B) N27 cells were exposed to endosulfan in the presence or absence of 50 nM of the autophagy inhibitor bafilomycin A1 for 6 h. The cell lysates were made and immunoblotting was analyzed for LC3 II. (C) The cells were treated with endosulfan (6–20 h) in the presence or absence of 50 nM wortmannin. Caspase-2 activity was measured by the fluorogenic caspase-2 substrate Ac-VDVAD-AFC. (D) N27 cells were treated with endosulfan (6 and 15 h) in the presence or absence of 50 nM bafilomycin A1. Caspase-2 activity was measured by the fluorogenic caspase-2 substrate Ac-VDVAD-AFC. (E) The cells were treated with endosulfan (6–20 h) with or without 50 nM wortmannin. Caspase-3 activity was measured by the fluorogenic caspase-3 substrate Ac-DEVD-AFC. (F) N27 cells were treated with endosulfan (6 and 15 h) with or without 50 nM bafilomycin A1. Caspase-2 activity was measured by the fluorogenic caspase-2 substrate Ac-VDVAD-AFC. (G–J) Cytotoxicity and cell viability were examined after 15-h treatment of endosulfan with or without wortmannin or bafilomycin A1 (50 nM) by SYTOX green fluorescence (G and H) or MTS assay (I and J), respectively. Asterisks (**$p < .01$; ***$p < .001$) indicate significant differences between wortmannin- or bafilomycin-co-treated and endosulfan-alone-treated cells.

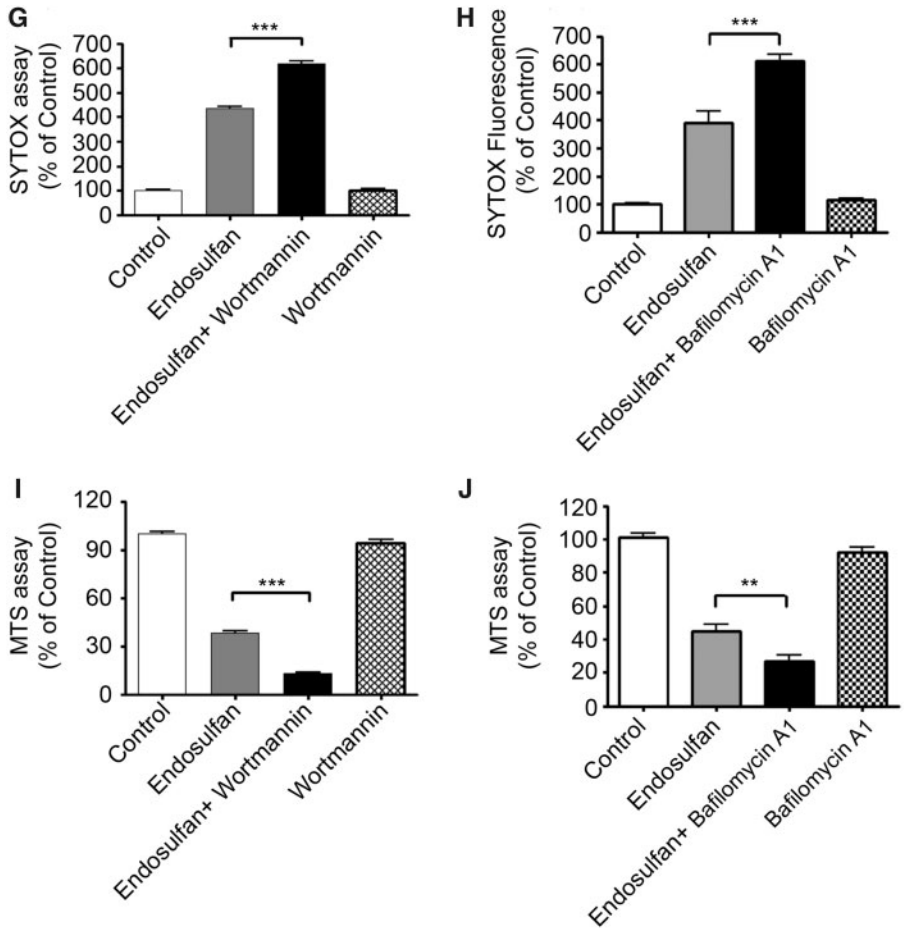

Figure 6. Continued

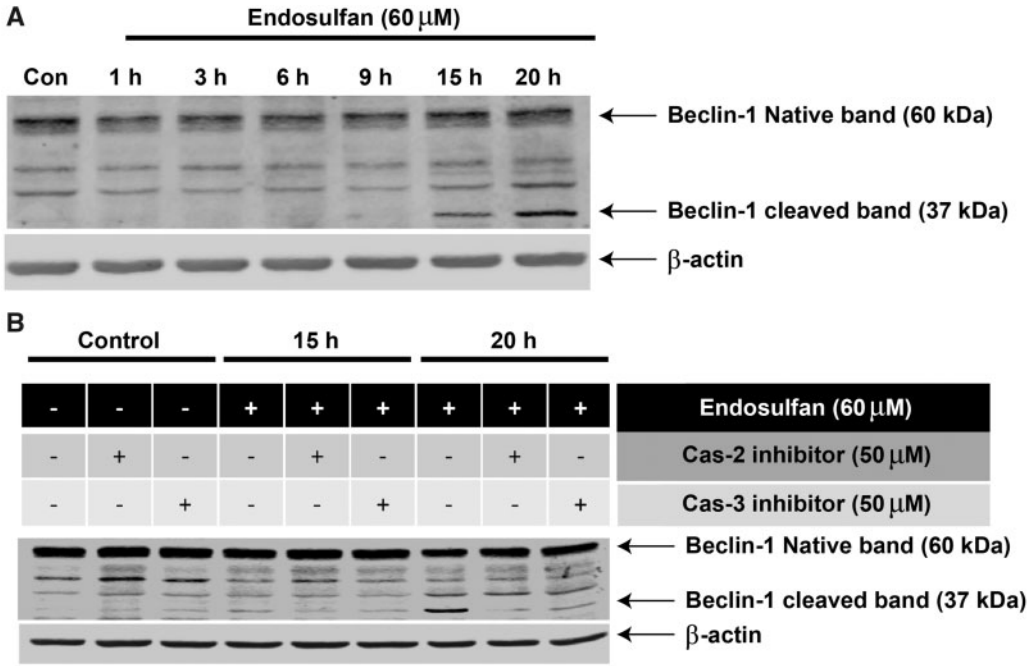

Figure 7. Beclin-1 is involved in endosulfan-induced autophagy and apoptosis. (A) N27 cells were treated with 60 μM endosulfan for 1, 3, 6, 9, 15 or 20 h. Beclin-1 cleavage was measured by immunoblotting cell lysates. Equal loading of protein was demonstrated using β-actin. (B) Western blot of N27 cells pretreated with 50 μM of a caspase-2 (Z-VDVAD-fmk) or caspase-3 inhibitor (Z-DEVD-fmk) for 1 h and then exposed to 60 μM endosulfan for 15 or 20 h. Equal loading of protein was demonstrated using β-actin.

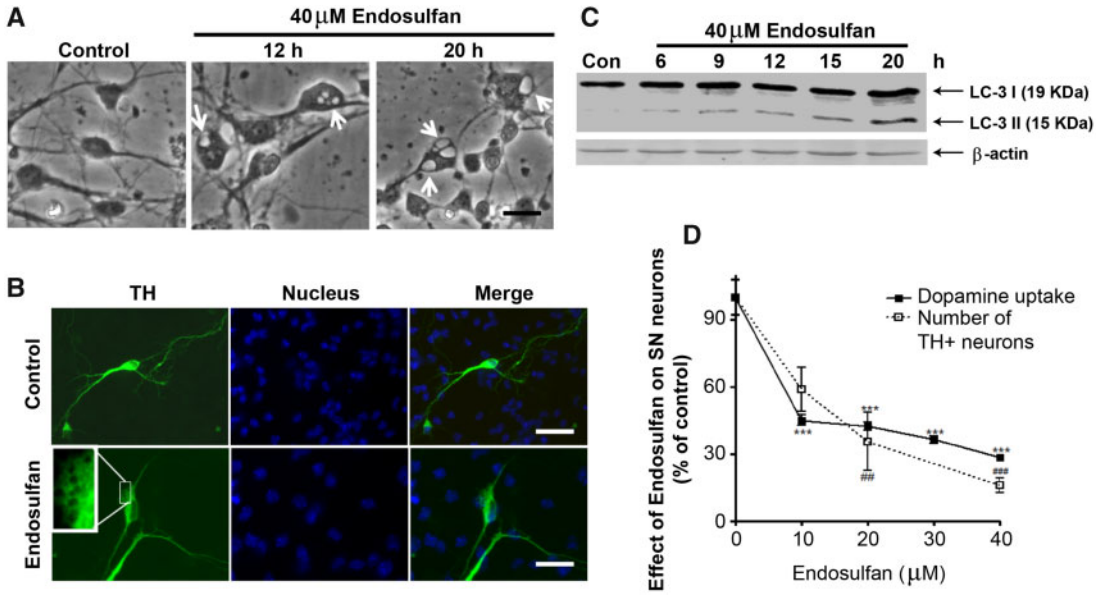

Figure 8. Endosulfan-induced autophagy and dopaminergic neuronal cell loss in primary mesencephalic cultures. (A) Primary cultures of striatal (STR) neurons were treated with 40 μM endosulfan for 12 or 20 h. Scale bar, 10 μm. Autophagic vacuoles were examined by phase-contrast microscopy. (B) Mesencephalic primary cultures were treated with 40 μM endosulfan for 20 h and morphological changes were examined, including autophagic vacuole formation. Scale bar, 10 μm. TH staining was used to define the TH+ dopaminergic neurons. (C) Immunoblot analyses of accumulating LC3-II protein in STR neurons treated with 40 μM endosulfan. β-actin expression was used as an equal loading control. (D) Assessment of viability of dopaminergic neurons using ^{3}H-DA uptake assay and the number of TH+ neurons. Asterisks (##, $p < .01$, *** and ###, $p < .001$) denote significant treatment effects relative to the vehicle-only dose (0 μM endosulfan).

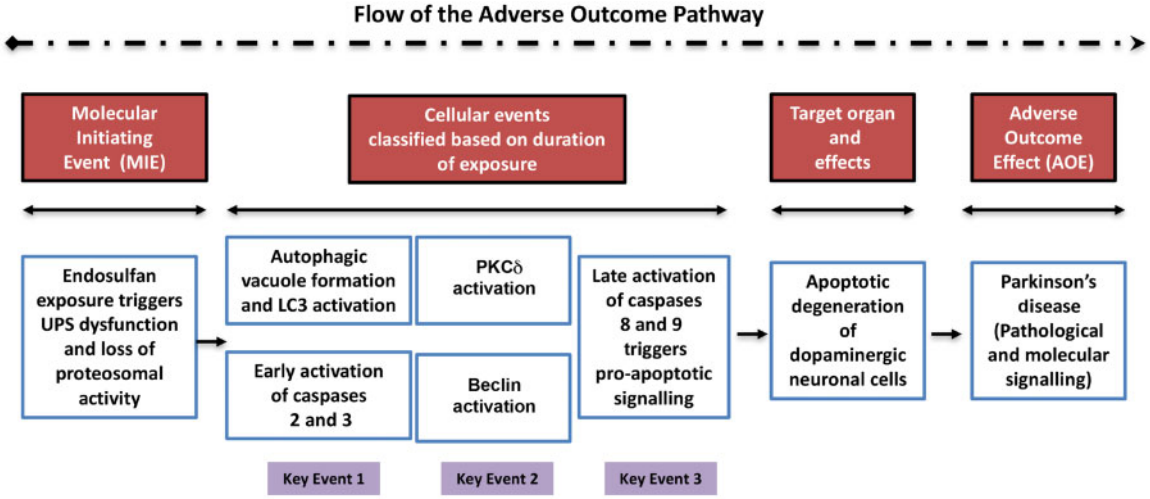

Figure 9. Adverse outcome pathway (AOP) highlighting the molecular mechanistic effects of endosulfan on dopaminergic neuronal cells. This AOP reiterates the mechanistic neurotoxic effects of endosulfan on dopaminergic neuronal cells. The line of events starts from the molecular initiating event, progresses sequentially to the cellular events (arranged to denote progression based on the duration of endosulfan treatment), then to the target organ-specific effects, and finally to the adverse outcome effect on dopaminergic neuronal cells post-endosulfan exposure. The cellular events are further subclassified and linked together as key events 1, 2, and 3.

early event, which is followed by apoptotic neuronal cell death after prolonged exposure. This endosulfan-induced autophagic response plays a protective role against endosulfan-mediated neurotoxicity and dopaminergic neuronal cell death. We also show that endosulfan-induced apoptosis is caspase-dependent, and caspase-2, as an initiator caspase acting upstream of the mitochondrial pathway, is of central importance. Furthermore, we also identify a potentially essential role of Beclin-1 cleavage in endosulfan-induced autophagy and neuronal cell loss. Our data vividly demonstrate the interplay between autophagy and apoptosis and shed light on the molecular mechanisms and signal cascades involved in environmental neurotoxicant-induced neurotoxicity and neuronal cell death (Figure 10). Our findings also advance the understanding of how autophagy, UPS, and apoptosis contribute to the pathogenesis of PD and may facilitate the development of promising therapeutic treatments for this devastating disease. Specifically, the search for an efficacious autophagy enhancer could be integrated into the development of potential PD therapies.

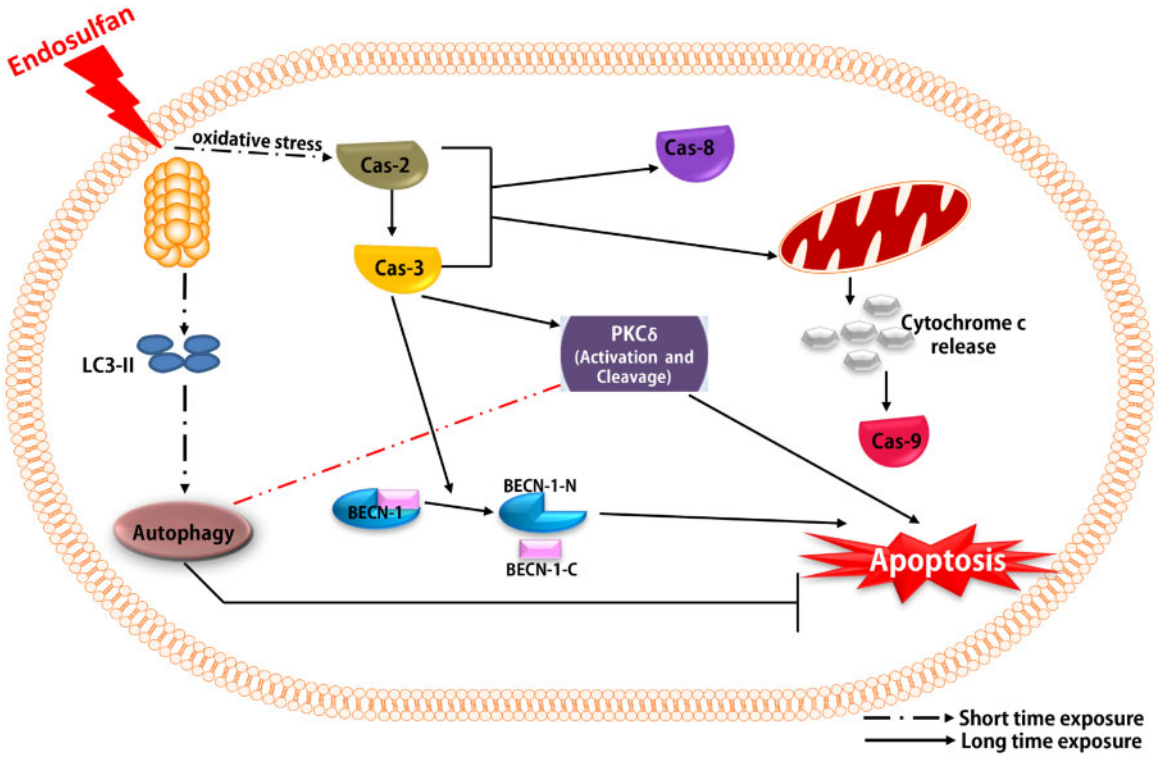

Figure 10. Schematic representation of mechanisms underlying endosulfan-induced autophagy and apoptosis. Exposure to the environmental neurotoxicant endosulfan instantly induces autophagic processes as an early response, followed by apoptotic cell death after prolonged treatment via activation of caspases and the mitochondrion-dependent pathway. Caspase-2, as an initial caspase, is a key upstream factor mediating endosulfan-induced cell apoptosis. Caspase-2 activates the executioner caspase-3. We clearly demonstrate that autophagy is a protective process that retards endosulfan-mediated cell death. Interestingly, we also provide evidence to show that Beclin-1 can be cleaved by caspases during endosulfan-induced cell apoptosis, suggesting a potentially important role of Beclin-1 in dopaminergic neuronal cell death. The autophagic response assumes a protective role against endosulfan-mediated neurotoxicity and dopaminergic neuronal cell death. We also show that endosulfan-induced apoptosis is caspase-dependent with caspase-2, as the initiator caspase, acting upstream of the mitochondria pathway, being of central importance. We also suggest a potentially essential role of Beclin-1 cleavage in endosulfan-induced neuronal cell loss.

SUPPLEMENTARY DATA

Supplementary data are available at *Toxicological Sciences* online.

DECLARATION OF CONFLICTING INTERESTS

A.G.K and V.A have an equity interest in PK Biosciences Corporation located in Ames, IA. The terms of this arrangement have been reviewed and approved by Iowa State University in accordance with its conflict of interest policies. Other authors declare no actual or potential competing financial interests.

ACKNOWLEDGMENTS

This work was supported by National Institutes of Health (NIH) (ES027245, ES026892, and NS045133). The W. E. Lloyd Endowed Chair and Eminent Scholar in Veterinary Medicine and Armbrust Endowment to A.G.K. and the Salisbury Endowed Chair to A.K. are also acknowledged. We also thank Gary Zenitsky for assistance in preparing this manuscript. This was presented at the Society of Toxicology 57th Annual meeting, Scientific Sessions symposium on Mechanisms of Autophagic Function and Dysfunction in Neurotoxicity and Neurodegeneration. A.G.K and V.A. have an equity interest in PK Biosciences Corporation located in Ames, Iowa. The terms of this arrangement have been reviewed and approved by Iowa State University in accordance with its conflict of interest policies. Other authors declare no actual or potential competing financial interests.

REFERENCES

Afeseh Ngwa, H., Kanthasamy, A., Gu, Y., Fang, N., Anantharam, V., and Kanthasamy, A. G. (2011). Manganese nanoparticle activates mitochondrial dependent apoptotic signaling and autophagy in dopaminergic neuronal cells. *Toxicol. Appl. Pharmacol.* **256**, 227–240.

Agrawal, A. K., Anand, M., Zaidi, N. F., and Seth, P. K. (1983). Involvement of serotonergic receptors in endosulfan neurotoxicity. *Biochem. Pharmacol.* **32**, 3591–3593.

Ahmed, T., Tripathi, A. K., Ahmed, R. S., Das, S., Suke, S. G., Pathak, R., Chakraboti, A., and Banerjee, B. D. (2008). Endosulfan-induced apoptosis and glutathione depletion in human peripheral blood mononuclear cells: Attenuation by N-acetylcysteine. *J. Biochem. Mol. Toxicol.* **22**, 299–304.

Aleksandrowicz, D. R. (1979). Endosulfan poisoning and chronic brain syndrome. *Arch. Toxicol.* **43**, 65–68.

Ansari, R., Husain, K., and Gupta, P. (1987). Endosulfan toxicity influence on biogenic amines of rat brain. *J. Environ. Biol.* **8**, 229–236.

Ansari, R. A., Siddiqui, M. K., and Gupta, P. K. (1984). Toxicity of endosulfan: Distribution of alpha- and beta-isomers of racemic endosulfan following oral administration in rats. *Toxicol. Lett.* **21**, 29–33.

Asaithambi, A., Ay, M., Jin, H., Gosh, A., Anantharam, V., Kanthasamy, A., and Kanthasamy, A. G. (2014). Protein kinase D1 (PKD1) phosphorylation promotes dopaminergic neuronal survival during 6-OHDA-induced oxidative stress. *PLoS One* **9**, e96947.

Biasini, E., Fioriti, L., Ceglia, I., Invernizzi, R., Bertoli, A., Chiesa, R., and Forloni, G. (2003). Proteasome inhibition and aggregation in Parkinson's disease: A comparative study in untransfected and transfected cells. *J. Neurochem.* **88**, 545–553.

Biederbick, A., Kern, H. F., and Elsasser, H. P. (1995). Monodansylcadaverine (MDC) is a specific in vivo marker for autophagic vacuoles. *Eur. J. Cell Biol.* **66**, 3–14.

Blanco-Coronado, J. L., Repetto, M., Ginestal, R. J., Vicente, J. R., Yelamos, F., and Lardelli, A. (1992). Acute intoxication by endosulfan. *J. Toxicol. Clin. Toxicol.* **30**, 575–583.

Blommaart, E. F., Krause, U., Schellens, J. P., Vreeling-Sindelarova, H., and Meijer, A. J. (1997). The phosphatidylinositol 3-kinase inhibitors wortmannin and LY294002 inhibit autophagy in isolated rat hepatocytes. *Eur. J. Biochem.* **243**, 240–246.

Boereboom, F. T., van Dijk, A., van Zoonen, P., and Meulenbelt, J. (1998). Nonaccidental endosulfan intoxication: A case report with toxicokinetic calculations and tissue concentrations. *J. Toxicol. Clin. Toxicol.* **36**, 345–352.

Bouchier-Hayes, L. (2010). The role of caspase-2 in stress-induced apoptosis. *J. Cell Mol. Med.* **14**, 1212–1224.

Boya, P., Gonzalez-Polo, R. A., Casares, N., Perfettini, J. L., Dessen, P., Larochette, N., Metivier, D., Meley, D., Souquere, S., Yoshimori, T., *et al.* (2005). Inhibition of macroautophagy triggers apoptosis. *Mol. Cell Biol.* **25**, 1025–1040.

Brandt, V. A., Moon, S., Ehlers, J., Methner, M. M., and Struttmann, T. (2001). Exposure to endosulfan in farmers: Two case studies. *Am. J. Ind. Med.* **39**, 643–649.

Brown, T. P., Rumsby, P. C., Capleton, A. C., Rushton, L., and Levy, L. S. (2006). Pesticides and Parkinson's disease–is there a link? *Environ. Health Perspect.* **114**, 156–164.

Chan, M. P., Morisawa, S., Nakayama, A., Kawamoto, Y., and Yoneda, M. (2006). Development of an in vitro blood-brain barrier model to study the effects of endosulfan on the permeability of tight junctions and a comparative study of the cytotoxic effects of endosulfan on rat and human glial and neuronal cell cultures. *Environ. Toxicol.* **21**, 223–235.

Charli, A., Jin, H., Anantharam, V., Kanthasamy, A., and Kanthasamy, A. G. (2016). Alterations in mitochondrial dynamics induced by tebufenpyrad and pyridaben in a dopaminergic neuronal cell culture model. *Neurotoxicology* **53**, 302–313.

Chen, J. L., Lin, H. H., Kim, K. J., Lin, A., Ou, J. H., and Ann, D. K. (2009). PKC delta signaling: A dual role in regulating hypoxic stress-induced autophagy and apoptosis. *Autophagy* **5**, 244–246.

Cheng, Y., Qiu, F., Huang, J., Tashiro, S., Onodera, S., and Ikejima, T. (2008). Apoptosis-suppressing and autophagy-promoting effects of calpain on oridonin-induced L929 cell death. *Arch. Biochem. Biophys.* **475**, 148–155.

Chhillar, N., Singh, N. K., Banerjee, B. D., Bala, K., Mustafa, M., Sharma, D., and Chhillar, M. (2013). Organochlorine pesticide levels and risk of Parkinson's disease in north Indian population. *ISRN Neurol.* **2013**, 1.

Cho, D. H., Jo, Y. K., Hwang, J. J., Lee, Y. M., Roh, S. A., and Kim, J. C. (2009). Caspase-mediated cleavage of ATG6/Beclin-1 links apoptosis to autophagy in HeLa cells. *Cancer Lett.* **274**, 95–100.

Dantuma, N. P., and Bott, L. C. (2014). The ubiquitin-proteasome system in neurodegenerative diseases: Precipitating factor, yet part of the solution. *Front Mol. Neurosci.* **7**, 70.

Demeter, J., Heyndrickx, A., Timperman, J., Lefevere, M., and De Beer, J. (1977). Toxicological analysis in a case of endosulfan suicide. *Bull Environ. Contam. Toxicol.* **18**, 110–114.

Dikshith, T. S., Raizada, R. B., Srivastava, M. K., and Kaphalia, B. S. (1984). Response of rats to repeated oral administration of endosulfan. *Ind. Health* **22**, 295–304.

Ding, W. X., Ni, H. M., Gao, W., Yoshimori, T., Stolz, D. B., Ron, D., and Yin, X. M. (2007). Linking of autophagy to ubiquitin-proteasome system is important for the regulation of endoplasmic reticulum stress and cell viability. *Am. J. Pathol.* **171**, 513–524.

Djavaheri-Mergny, M., Maiuri, M. C., and Kroemer, G. (2010). Cross talk between apoptosis and autophagy by caspase-mediated cleavage of Beclin 1. *Oncogene* **29**, 1717–1719.

Du, H., Wang, M., Wang, L., Dai, H., Wang, M., Hong, W., Nie, X., Wu, L., and Xu, A. (2015). Reproductive toxicity of endosulfan: Implication from germ cell apoptosis modulated by mitochondrial dysfunction and genotoxic Response Genes in *Caenorhabditis elegans*. *Toxicol. Sci.* **145**, 118–127.

Emoto, Y., Manome, Y., Meinhardt, G., Kisaki, H., Kharbanda, S., Robertson, M., Ghayur, T., Wong, W. W., Kamen, R., and Weichselbaum, R. (1995). Proteolytic activation of protein kinase C delta by an ICE-like protease in apoptotic cells. *EMBO J.* **14**, 6148–6156.

Eyer, F., Felgenhauer, N., Jetzinger, E., Pfab, R., and Zilker, T. R. (2004). Acute endosulfan poisoning with cerebral edema and cardiac failure. *J. Toxicol. Clin. Toxicol.* **42**, 927–932.

Fleming, L., Mann, J. B., Bean, J., Briggle, T., and Sanchez-Ramos, J. R. (1994). Parkinson's disease and brain levels of organochlorine pesticides. *Ann. Neurol.* **36**, 100–103.

Fleming, S. M. (2017). Mechanisms of gene-environment interactions in Parkinson's disease. *Curr. Environ. Health Rep.* **4**, 192–199.

Furuya, N., Yu, J., Byfield, M., Pattingre, S., and Levine, B. (2005). The evolutionarily conserved domain of Beclin 1 is required for Vps34 binding, autophagy and tumor suppressor function. *Autophagy* **1**, 46–52.

Galluzzi, L., Vicencio, J. M., Kepp, O., Tasdemir, E., Maiuri, M. C., and Kroemer, G. (2008). To die or not to die: That is the autophagic question. *Curr. Mol. Med.* **8**, 78–91.

Gozuacik, D., and Kimchi, A. (2004). Autophagy as a cell death and tumor suppressor mechanism. *Oncogene* **23**, 2891–2906.

Green, D. R., and Reed, J. C. (1998). Mitochondria and apoptosis. *Science* **281**, 1309–1312.

Gude, D., and Bansal, D. P. (2012). Revisiting endosulfan. *J. Family Med. Prim. Care* **1**, 76–78.

Gupta, P. K. (1978). Distribution of endosulfan in plasma and brain after repeated oral administration to rats. *Toxicology* **9**, 371–377.

Harvey, N. L., Butt, A. J., and Kumar, S. (1997). Functional activation of Nedd2/ICH-1 (caspase-2) is an early process in apoptosis. *J. Biol. Chem.* **272**, 13134–13139.

Hatcher, J. M., Pennell, K. D., and Miller, G. W. (2008). Parkinson's disease and pesticides: A toxicological perspective. *Trends Pharmacol. Sci.* **29**, 322–329.

Hatcher, J. M., Richardson, J. R., Guillot, T. S., McCormack, A. L., Di Monte, D. A., Jones, D. P., Pennell, K. D., and Miller, G. W. (2007). Dieldrin exposure induces oxidative damage in the mouse nigrostriatal dopamine system. *Exp. Neurol.* **204**, 619–630.

Jang, T. C., Jang, J. H., and Lee, K. W. (2016). Mechanism of acute endosulfan intoxication-induced neurotoxicity in Sprague-Dawley rats. *Arh. Hig. Rada. Toksikol.* **67**, 9–17.

Jia, Z., and Misra, H. P. (2007a). Developmental exposure to pesticides zineb and/or endosulfan renders the nigrostriatal dopamine system more susceptible to these environmental chemicals later in life. *Neurotoxicology* **28**, 727–735.

Jia, Z., and Misra, H. P. (2007b). Exposure to mixtures of endosulfan and zineb induces apoptotic and necrotic cell death in SH-SY5Y neuroblastoma cells, in vitro. *J. Appl. Toxicol.* **27**, 434–446.

Jia, Z., and Misra, H. P. (2007c). Reactive oxygen species in in vitro pesticide-induced neuronal cell (SH-SY5Y) cytotoxicity: Role of NFkappaB and caspase-3. *Free Radic Biol. Med.* **42**, 288–298.

Jin, H., Kanthasamy, A., Harischandra, D. S., Kondru, N., Ghosh, A., Panicker, N., Anantharam, V., Rana, A., and Kanthasamy, A. G. (2014). Histone hyperacetylation up-regulates protein kinase Cδ in dopaminergic neurons to induce cell death: Relevance to epigenetic mechanisms of neurodegeneration in Parkinson disease. *J. Biol. Chem.* **289**, 34743–34767.

Kabeya, Y., Mizushima, N., Ueno, T., Yamamoto, A., Kirisako, T., Noda, T., Kominami, E., Ohsumi, Y., and Yoshimori, T. (2000). LC3, a mammalian homologue of yeast Apg8p, is localized in autophagosome membranes after processing. *EMBO J.* **19**, 5720–5728.

Kang, K. S., Park, J. E., Ryu, D. Y., and Lee, Y. S. (2001). Effects and neuro-toxic mechanisms of 2,2',4,4',5,5'-hexachlorobiphenyl and endosulfan in neuronal stem cells. *J. Vet. Med. Sci.* **63**, 1183–1190.

Kannan, K., Holcombe, R. F., Jain, S. K., Alvarez-Hernandez, X., Chervenak, R., Wolf, R. E., and Glass, J. (2000). Evidence for the induction of apoptosis by endosulfan in a human T-cell leukemic line. *Mol. Cell Biochem.* **205**, 53–66.

Kannan, K., and Jain, S. K. (2003). Oxygen radical generation and endosulfan toxicity in Jurkat T-cells. *Mol. Cell Biochem.* **247**, 1–7.

Kanthasamy, A., Jin, H., Anantharam, V., Sondarva, G., Rangasamy, V., Rana, A., and Kanthasamy, A. (2012). Emerging neurotoxic mechanisms in environmental factors-induced neurodegeneration. *Neurotoxicology* **33**, 833–837.

Kanthasamy, A. G., Anantharam, V., Zhang, D., Latchoumycandane, C., Jin, H., Kaul, S., and Kanthasamy, A. (2006). A novel peptide inhibitor targeted to caspase-3 cleavage site of a proapoptotic kinase protein kinase C delta (PKCdelta) protects against dopaminergic neuronal degeneration in Parkinson's disease models. *Free Radic. Biol. Med.* **41**, 1578–1589.

Kanthasamy, A. G., Kitazawa, M., Kanthasamy, A., and Anantharam, V. (2003). Role of proteolytic activation of protein kinase Cdelta in oxidative stress-induced apoptosis. *Antioxid. Redox. Signal.* **5**, 609–620.

Kanthasamy, A. G., Kitazawa, M., Kanthasamy, A., and Anantharam, V. (2005). Dieldrin-induced neurotoxicity: Relevance to Parkinson's disease pathogenesis. *Neurotoxicology* **26**, 701–719.

Kaul, S., Anantharam, V., Yang, Y., Choi, C. J., Kanthasamy, A., and Kanthasamy, A. G. (2005). Tyrosine phosphorylation regulates the proteolytic activation of protein kinase Cdelta in dopaminergic neuronal cells. *J. Biol. Chem.* **280**, 28721–28730.

Kaul, S., Kanthasamy, A., Kitazawa, M., Anantharam, V., and Kanthasamy, A. G. (2003). Caspase-3 dependent proteolytic activation of protein kinase C delta mediates and regulates 1-methyl-4-phenylpyridinium (MPP+)-induced apoptotic cell death in dopaminergic cells: Relevance to oxidative stress in dopaminergic degeneration. *Eur. J. Neurosci.* **18**, 1387–1401.

Kelly, B. C., and Gobas, F. A. (2003). An arctic terrestrial food-chain bioaccumulation model for persistent organic pollutants. *Environ. Sci. Technol.* **37**, 2966–2974.

Kihara, A., Kabeya, Y., Ohsumi, Y., and Yoshimori, T. (2001). Beclin-phosphatidylinositol 3-kinase complex functions at the trans-Golgi network. *EMBO Rep.* **2**, 330–335.

Kim, K., Jeon, H. J., Choi, S. D., Tsang, D. C. W., Oleszczuk, P., Ok, Y. S., Lee, H. S., and Lee, S. E. (2018). Combined toxicity of endosulfan and phenanthrene mixtures and induced molecular changes in adult Zebrafish (*Danio rerio*). *Chemosphere* **194**, 30–41.

Kitazawa, M., Anantharam, V., and Kanthasamy, A. G. (2001). Dieldrin-induced oxidative stress and neurochemical changes contribute to apoptopic cell death in dopaminergic cells. *Free Radic. Biol. Med.* **31**, 1473–1485.

Kitazawa, M., Anantharam, V., and Kanthasamy, A. G. (2003). Dieldrin induces apoptosis by promoting caspase-3-dependent proteolytic cleavage of protein kinase Cdelta in dopaminergic cells: Relevance to oxidative stress and dopaminergic degeneration. *Neuroscience* **119**, 945–964.

Kitazawa, M., Anantharam, V., Kanthasamy, A., and Kanthasamy, A. G. (2004). Dieldrin promotes proteolytic cleavage of poly(ADP-ribose) polymerase and apoptosis in dopaminergic cells: Protective effect of mitochondrial anti-apoptotic protein Bcl-2. *Neurotoxicology* **25**, 589–598.

Klionsky, D. J., Elazar, Z., Seglen, P. O., and Rubinsztein, D. C. (2008). Does bafilomycin A1 block the fusion of autophagosomes with lysosomes? *Autophagy* **4**, 849–850.

Klionsky, D. J., and Emr, S. D. (2000). Autophagy as a regulated pathway of cellular degradation. *Science* **290**, 1717–1721.

Kroemer, G., and Reed, J. C. (2000). Mitochondrial control of cell death. *Nat. Med.* **6**, 513–519.

Krumschnabel, G., Sohm, B., Bock, F., Manzl, C., and Villunger, A. (2009). The enigma of caspase-2: The laymen's view. *Cell Death Differ.* **16**, 195–207.

Kucuker, H., Sahin, O., Yavuz, Y., and Yurumez, Y. (2009). Fatal acute endosulfan toxicity: A case report. *Basic Clin. Pharmacol. Toxicol.* **104**, 49–51.

Kumari, U., Srivastava, N., Shelly, A., Khatri, P., N, S., Singh, D. K., and Mazumder, S. (2016). Inducible headkidney cytochrome P450 contributes to endosulfan immunotoxicity in walking catfish *Clarias gariepinus*. *Aquat. Toxicol.* **179**, 44–54.

Kuribayashi, K., Mayes, P. A., and El-Deiry, W. S. (2006). What are caspases 3 and 7 doing upstream of the mitochondria? *Cancer Biol. Ther.* **5**, 763–765.

Lafuente, A., and Pereiro, N. (2013). Neurotoxic effects induced by endosulfan exposure during pregnancy and lactation in female and male rat striatum. *Toxicology* **311**, 35–40.

Lakroun, Z., Kebieche, M., Lahouel, A., Zama, D., Desor, F., and Soulimani, R. (2015). Oxidative stress and brain mitochondria swelling induced by endosulfan and protective role of quercetin in rat. *Environ. Sci. Pollut Res. Int.* **22**, 7776–7781.

Latchoumycandane, C., Anantharam, V., Kitazawa, M., Yang, Y., Kanthasamy, A., and Kanthasamy, A. G. (2004). Protein kinase Cdelta is a key downstream mediator of manganese-induced apoptosis in dopaminergic neuronal cells. *J. Pharmacol. Exp. Ther.* **313**, 46–55.

Lee, I., Eriksson, P., Fredriksson, A., Buratovic, S., and Viberg, H. (2015). Developmental neurotoxic effects of two pesticides: Behavior and neuroprotein studies on endosulfan and cypermethrin. *Toxicology* **335**, 1–10.

Lee, J. A. (2009). Autophagy in neurodegeneration: Two sides of the same coin. *BMB Rep*. **42**, 324–330.

Levine, B., and Deretic, V. (2007). Unveiling the roles of autophagy in innate and adaptive immunity. *Nat. Rev. Immunol.* **7**, 767–777.

Levine, B., and Yuan, J. (2005). Autophagy in cell death: An innocent convict? *J. Clin. Invest.* **115**, 2679–2688.

Li, C., Guo, Y., Xie, W., Li, X., Janokovic, J., and Le, W. (2010). Neuroprotection of pramipexole in UPS impairment induced animal model of Parkinson's disease. *Neurochem. Res.* **35**, 1546?1556.

Li, H., Bergeron, L., Cryns, V., Pasternack, M. S., Zhu, H., Shi, L., Greenberg, A., and Yuan, J. (1997). Activation of caspase-2 in apoptosis. *J. Biol. Chem.* **272**, 21010–21017.

Liang, X. H., Jackson, S., Seaman, M., Brown, K., Kempkes, B., Hibshoosh, H., and Levine, B. (1999). Induction of autophagy and inhibition of tumorigenesis by beclin 1. *Nature* **402**, 672–676.

Lin, C. F., Chen, C. L., Chang, W. T., Jan, M. S., Hsu, L. J., Wu, R. H., Tang, M. J., Chang, W. C., and Lin, Y. S. (2004). Sequential caspase-2 and caspase-8 activation upstream of mitochondria during ceramideand etoposide-induced apoptosis. *J. Biol. Chem.* **279**, 40755–40761.

Lubick, N. (2010). Environment. Endosulfan's exit: U.S. EPA pesticide review leads to a ban. *Science* **328**, 1466.

Luo, S., and Rubinsztein, D. C. (2010). Apoptosis blocks Beclin 1-dependent autophagosome synthesis: An effect rescued by Bcl-xL. *Cell Death Differ.* **17**, 268–277.

Maiuri, M. C., Criollo, A., and Kroemer, G. (2010). Crosstalk between apoptosis and autophagy within the Beclin 1 interactome. *EMBO J.* **29**, 515–516.

Martins-Branco, D., Esteves, A. R., Santos, D., Arduino, D. M., Swerdlow, R. H., Oliveira, C. R., Januario, C., and Cardoso, S. M. (2012). Ubiquitin proteasome system in Parkinson's disease: A keeper or a witness? *Exp. Neurol.* **238**, 89–99.

Matsuda, N., and Tanaka, K. (2010). Does impairment of the ubiquitin-proteasome system or the autophagy-lysosome pathway predispose individuals to neurodegenerative disorders such as Parkinson's disease? *J. Alzheimers Dis.* **19**, 1–9.

Menezes, R. G., Qadir, T. F., Moin, A., Fatima, H., Hussain, S. A., Madadin, M., Pasha, S. B., Al Rubaish, F. A., and Senthilkumaran, S. (2017). Endosulfan poisoning: An overview. *J. Forensic Leg. Med.* **51**, 27–33.

Munafo, D. B., and Colombo, M. I. (2001). A novel assay to study autophagy: Regulation of autophagosome vacuole size by amino acid deprivation. *J. Cell Sci.* **114**, 3619–3629.

Naqvi, S. M., and Vaishnavi, C. (1993). Bioaccumulative potential and toxicity of endosulfan insecticide to non-target animals. *Comp. Biochem. Physiol. C.* **105**, 347–361.

Nixon, R. A. (2006). Autophagy in neurodegenerative disease: Friend, foe or turncoat? *Trends Neurosci.* **29**, 528–535.

Oliveira, J. M., Brinati, A., Miranda, L. D. L., Morais, D. B., Zanuncio, J. C., Goncalves, R. V., Peluzio, M., and Freitas, M. B. (2017). Exposure to the insecticide endosulfan induces liver morphology alterations and oxidative stress in fruit-eating bats (*Artibeus lituratus*). *Int. J. Exp. Pathol.* **98**, 17–25.

Pan, T., Rawal, P., Wu, Y., Xie, W., Jankovic, J., and Le, W. (2009). Rapamycin protects against rotenone-induced apoptosis through autophagy induction. *Neuroscience* **164**, 541–551.

Paul, V., and Balasubramaniam, E. (1997). Effects of single and repeated administration of endosulfan on behaviour and its interaction with centrally acting drugs in experimental animals: A mini review. *Environ. Toxicol. Pharmacol.* **3**, 151–157.

Paul, V., Balasubramaniam, E., and Kazi, M. (1994). The neurobehavioural toxicity of endosulfan in rats: A serotonergic involvement in learning impairment. *Eur. J. Pharmacol.* **270**, 1–7.

Ponzoni, L., Moretti, M., Sala, M., Fasoli, F., Mucchietto, V., Lucini, V., Cannazza, G., Gallesi, G., Castellana, C. N., Clementi, F., *et al*. (2015). Different physiological and behavioural effects of e-cigarette vapour and cigarette smoke in mice. *Eur. Neuropsychopharmacol.* **25**, 1775–1786.

Rainey, N. E., Saric, A., Leberre, A., Dewailly, E., Slomianny, C., Vial, G., Zeliger, H. I., and Petit, P. X. (2017). Synergistic cellular effects including mitochondrial destabilization, autophagy and apoptosis following low-level exposure to a mixture of lipophilic persistent organic pollutants. *Sci. Rep.* **7**, 4728.

Read, S. H., Baliga, B. C., Ekert, P. G., Vaux, D. L., and Kumar, S. (2002). A novel Apaf-1-independent putative caspase-2 activation complex. *J. Cell Biol.* **159**, 739–745.

Redmann, M., Benavides, G. A., Berryhill, T. F., Wani, W. Y., Ouyang, X., Johnson, M. S., Ravi, S., Barnes, S., Darley-Usmar, V. M., and Zhang, J. (2017). Inhibition of autophagy with bafilomycin and chloroquine decreases mitochondrial quality and bioenergetic function in primary neurons. *Redox Biol.* **11**, 73–81.

Ren, N. Q., Zhang, X. D., Zhou, G. H., and Chen, S. J. (2008). [Induced apoptosis and mechanism of endosulfan in mouse germ cells]. *Huan Jing Ke Xue* **29**, 386–390.

Ribeiro, S., Sousa, J. P., Nogueira, A. J., and Soares, A. M. (2001). Effect of endosulfan and parathion on energy reserves and physiological parameters of the terrestrial isopod *Porcellio dilatatus*. *Ecotoxicol. Environ. Saf.* **49**, 131–138.

Richardson, J. R., Caudle, W. M., Wang, M., Dean, E. D., Pennell, K. D., and Miller, G. W. (2006). Developmental exposure to the pesticide dieldrin alters the dopamine system and increases neurotoxicity in an animal model of Parkinson's disease. *FASEB J.* **20**, 1695–1697.

Rideout, H. J., and Stefanis, L. (2002). Proteasomal inhibition-induced inclusion formation and death in cortical neurons require transcription and ubiquitination. *Mol. Cell Neurosci.* **21**, 223–238.

Robertson, J. D., and Orrenius, S. (2000). Molecular mechanisms of apoptosis induced by cytotoxic chemicals. *Crit. Rev. Toxicol.* **30**, 609–627.

Sarkar, S., Malovic, E., Harishchandra, D. S., Ghaisas, S., Panicker, N., Charli, A., Palanisamy, B. N., Rokad, D., Jin, H., and Anantharam, V. (2017). Mitochondrial impairment in microglia amplifies NLRP3 inflammasome proinflammatory signaling in cell culture and animal models of Parkinson's disease. *NPJ Parkinsons Dis.* **3**, 30.

Scott, R. C., Juhasz, G., and Neufeld, T. P. (2007). Direct induction of autophagy by Atg1 inhibits cell growth and induces apoptotic cell death. *Curr. Biol.* **17**, 1–11.

Seth, P. K., Saidi, N. F., Agrawal, A. K., and Anand, M. (1986). Neurotoxicity of endosulfan in young and adult rats. *Neurotoxicology* **7**, 623–635.

Shacka, J. J., Klocke, B. J., Shibata, M., Uchiyama, Y., Datta, G., Schmidt, R. E., and Roth, K. A. (2006). Bafilomycin A1 inhibits chloroquine-induced death of cerebellar granule neurons. *Mol. Pharmacol.* **69**, 1125–1136.

Sherer, T. B., Betarbet, R., Stout, A. K., Lund, S., Baptista, M., Panov, A. V., Cookson, M. R., and Greenamyre, J. T. (2002). An in vitro model of Parkinson's disease: Linking mitochondrial impairment to altered alpha-synuclein metabolism and oxidative damage. *J. Neurosci.* **22**, 7006–7015.

Silva, M. H., and Gammon, D. (2009). An assessment of the developmental, reproductive, and neurotoxicity of endosulfan. *Birth Defects Res. B. Dev. Reprod. Toxicol.* **86**, 1–28.

Singh, N., Lawana, V., Luo, J., Phong, P., Abdalla, A., Palanisamy, B., Rokad, D., Sarkar, S., Jin, H., Anantharam, V., *et al.* (2018). Organophosphate pesticide chlorpyrifos impairs STAT1 signaling to induce dopaminergic neurotoxicity: Implications for mitochondria mediated oxidative stress signaling events. *Neurobiol. Dis.* **117**, 82–113.

Song, C., Kanthasamy, A., Anantharam, V., Sun, F., and Kanthasamy, A. G. (2010). Environmental neurotoxic pesticide increases histone acetylation to promote apoptosis in dopaminergic neuronal cells: Relevance to epigenetic mechanisms of neurodegeneration. *Mol. Pharmacol.* **77**, 621–632.

Sun, F., Anantharam, V., Latchoumycandane, C., Kanthasamy, A., and Kanthasamy, A. G. (2005). Dieldrin induces ubiquitin-proteasome dysfunction in alpha-synuclein overexpressing dopaminergic neuronal cells and enhances susceptibility to apoptotic cell death. *J. Pharmacol. Exp. Ther.* **315**, 69–79.

Sun, F., Anantharam, V., Zhang, D., Latchoumycandane, C., Kanthasamy, A., and Kanthasamy, A. G. (2006). Proteasome inhibitor MG-132 induces dopaminergic degeneration in cell culture and animal models. *Neurotoxicology* **27**, 807–815.

Sun, F., Kanthasamy, A., Song, C., Yang, Y., Anantharam, V., and Kanthasamy, A. G. (2008). Proteasome inhibitor-induced apoptosis is mediated by positive feedback amplification of PKCdelta proteolytic activation and mitochondrial translocation. *J. Cell Mol. Med.* **12**, 2467–2481.

Sy, L. K., Yan, S. C., Lok, C. N., Man, R. Y., and Che, C. M. (2008). Timosaponin A-III induces autophagy preceding mitochondria-mediated apoptosis in HeLa cancer cells. *Cancer Res.* **68**, 10229–10237.

Tanida, I., Yamaji, T., Ueno, T., Ishiura, S., Kominami, E., and Hanada, K. (2008). Consideration about negative controls for LC3 and expression vectors for four colored fluorescent protein-LC3 negative controls. *Autophagy* **4**, 131–134.

Tanner, C. M., and Ben-Shlomo, Y. (1999). Epidemiology of Parkinson's disease. *Adv. Neurol.* **80**, 153–159.

Wang, N., Qian, H. Y., Zhou, X. Q., Li, Y. B., and Sun, Z. W. (2012). Mitochondrial energy metabolism dysfunction involved in reproductive toxicity of mice caused by endosulfan and protective effects of vitamin E. *Ecotoxicol. Environ. Saf.* **82**, 96–103.

Wilson, M. R. (1998). Apoptosis: Unmasking the executioner. *Cell Death Differ.* **5**, 646–652.

Wilson, W. W., Shapiro, L. P., Bradner, J. M., and Caudle, W. M. (2014). Developmental exposure to the organochlorine insecticide endosulfan damages the nigrostriatal dopamine system in male offspring. *Neurotoxicology* **44**, 279–287.

Winslow, A. R., and Rubinsztein, D. C. (2008). Autophagy in neurodegeneration and development. *Biochim. Biophys. Acta.* **1782**, 723–729.

Wirawan, E., Walle, L. V., Kersse, K., Cornelis, S., Claerhout, S., Vanoverberghe, I., Roelandt, R., Rycke, R. D., Verspurten, J., Declercq, W., *et al.* (2010). Caspase-mediated cleavage of Beclin-1 inactivates Beclin-1-induced autophagy and enhances apoptosis by promoting the release of proapoptotic factors from mitochondria. *Cell Death Dis.* **1**, e18.

Wong, E., and Cuervo, A. M. (2010). Autophagy gone awry in neurodegenerative diseases. *Nat. Neurosci.* **13**, 805–811.

Yu, L., Wan, F., Dutta, S., Welsh, S., Liu, Z., Freundt, E., Baehrecke, E. H., and Lenardo, M. (2006). Autophagic programmed cell death by selective catalase degradation. *Proc. Natl. Acad. Sci. U.S.A.* **103**, 4952–4957.

Zervos, I. A., Nikolaidis, E., Lavrentiadou, S. N., Tsantarliotou, M. P., Eleftheriadou, E. K., Papapanagiotou, E. P., Fletouris, D. J., Georgiadis, M., and Taitzoglou, I. A. (2011). Endosulfan-induced lipid peroxidation in rat brain and its effect on t-PA and PAI-1: Ameliorating effect of vitamins C and E. *J. Toxicol. Sci.* **36**, 423–433.

Zhang, D., Kanthasamy, A., Yang, Y., Anantharam, V., and Kanthasamy, A. (2007). Protein kinase C delta negatively regulates tyrosine hydroxylase activity and dopamine synthesis by enhancing protein phosphatase-2A activity in dopaminergic neurons. *J. Neurosci.* **27**, 5349–5362.

Zhang, D., Pan, J., Xiang, X., Liu, Y., Dong, G., Livingston, M. J., Chen, J. K., Yin, X. M., and Dong, Z. (2017a). Protein kinase Cdelta suppresses autophagy to induce kidney cell apoptosis in cisplatin nephrotoxicity. *J. Am. Soc. Nephrol.* **28**, 1131–1144.

Zhang, L., Wei, J., Ren, L., Zhang, J., Wang, J., Jing, L., Yang, M., Yu, Y., Sun, Z., and Zhou, X. (2017b). Endosulfan induces autophagy and endothelial dysfunction via the AMPK/mTOR signaling pathway triggered by oxidative stress. *Environ. Pollut.* **220(**Pt B), 843–852.

Zheng, Q., Li, J., and Wang, X. (2009). Interplay between the ubiquitin-proteasome system and autophagy in proteinopathies. *Int. J. Physiol. Pathophysiol. Pharmacol.* **1**, 127–142.